Low-Complexity Methods to Mitigate the Impact of Environmental Variables on Low-Cost UAS-based Atmospheric Carbon Dioxide Measurements

Gustavo B. H. de Azevedo[1,2*], Bill Doyle[2], Christopher A. Fiebrich[3], and David Schvartzman[1,4]

[1]Advanced Radar Research Center (ARRC) at The University of Oklahoma
[2]Center for Autonomous Sensing and Sampling (CASS) at The University of Oklahoma
[3]Oklahoma Mesonet, Oklahoma Climatological Survey at The University of Oklahoma
[4]School of Meteorology at The University of Oklahoma

Correspondence: Gustavo B. H. de Azevedo (gust@ou.edu)

Abstract. This article assesses the individual and joint impact of pressure, temperature, and relative humidity on the accuracy of atmospheric CO_2 measurements collected by Unmanned Aerial Systems (UAS) using low-cost commercial Non-Dispersive Infrared sensors (NDIR). We build upon previous experimental results in the literature and ~~systematically increase the variation range~~ present a new dataset with increased gradients for each environmental variable to match the abrupt changes found in ~~UAS~~ UAS-based atmospheric vertical profiles. As a key contribution, we present a ~~low-cost benchtop~~ low-complexity correction procedure to mitigate the impact of these variables and ~~considerably~~ improve the accuracy of ~~CO_2 measurements to be within ± 2.5~~ this type of atmospheric CO_2 measurement. Our findings support the use of low-cost NDIR sensors for UAS-based atmospheric CO_2 measurements as a complementary in-situ tool for many scientific applications.

1 Introduction

Over the past ~~60 years, atmospheric Carbon Dioxide (CO_2) has been measured with instrumented towers, satellites, and manned aircraft. During this period, these measurement systems provided insight into global concentration trends, continental fluxes, and other large scale behaviors (Kunz et al., 2018). In recent years atmospheric CO_2 studies have shifted focus from global and continental scales to finer regional and local scales (i.e., mesoscale, 2 to 20 , minutes to hours, Stephens et al., 2011). These new regional studies demonstrated how the mentioned measurement systems do not always support fast and comprehensive data collection near regional and local phenomena. Over the past~~ two decades, Unmanned Aerial Systems (UAS) have grown as a complementary in-situ observation tool for local atmospheric CO_2 profiles (Villa et al., 2016). This growth is justified by the relatively low cost of UAS and its ability to provide atmospheric CO_2 measurements with high spatiotemporal resolution

*Gustavo B. H. de Azevedo is now with the Unmanned Systems Research Institute at Oklahoma State University (OSU). Email: gus@okstate.edu

(Piedrahita et al., 2014). In a literature survey, Villa et al. (2016) ~~also highlights~~ highlight other motivations, such as in-situ validation of remote instruments, autonomous plume tracking, and locating hazardous emission sources.

In many of ~~the applicationsmentioned above~~these applications, the low-cost aspect of UAS-based solutions is ~~a crucial element~~ crucial to the application's feasibility (Nelson et al., 2019; Cartier, 2019; Kunz et al., 2018; Martin et al., 2017; Mitchell et al., 2016; Kiefer et al., 2012; Yasuda et al., 2008; Watai et al., 2006). In addition, the sensor's size, weight, and power requirements ~~of sensors~~ are also critical to the design of UAS-based solutions (Martin et al., 2017). For these reasons, many UAS-based atmospheric CO_2 measurement systems use commercial low-cost Non-Dispersive Infrared (NDIR) sensors (B. H. de Azevedo, 2020; Kunz et al., 2018; Martin et al., 2017; Gibson and MacGregor, 2013; Stephens et al., 2011; Yasuda et al., 2008; Pandey and Kim, 2007; Watai et al., 2006; Chen et al., 2002). However, abrupt changes in pressure, temperature, and relative humidity associated with atmospheric vertical profiles can interfere with ~~NDIR~~ low-cost NDIR CO_2 sensors.

In this article, we ~~begin by briefly reviewing~~ review the main concerns regarding the use of commercial low-cost NDIR sensors for atmospheric CO_2 measurements found in the literature. We then build upon previous experimental results in the literature by investigating the impact of each environmental variable on ~~the measured CO_2 while systematically increasing their absolute values. Finally, we evaluate the performance of a~~ low-cost ~~NDIR sensor under a wide range of conditions. As a key contribution of this article, we propose~~ NDIR CO_2 sensors. We also present a new dataset with stronger rates of change than previously found in the literature. These stronger rates of change are obtained by increasing the span of change in the test variables and decreasing experimental time scales. Finally, we evaluate if a set of low-cost benchtop procedures ~~that~~ can be used to characterize and mitigate the impact of these variables on the same ~~sensor.~~ sensors. All the experiments in this article were performed with low-complexity and repeatable methods. These methods used reference gas analyzers, non-gas specialized environmental chambers, and resources accessible to most researchers. The methods demonstrated were capable of correcting the measurements of low-cost NDIR sensors to a few ppm of more expensive reference benchtop gas analyzers. We believe these ~~low-cost procedures can be used by the scientific community to improve~~ low-complexity procedures are a way to lower the entry barriers to this research field while improving the accuracy of UAS-based CO_2 measurements~~and increase assimilation of UAS-based CO_2 datasets by atmospheric scientists~~.

1.1 Background and Motivation

Many low-cost ~~NDIR-based~~ NDIR CO_2 sensors are available ~~in~~ on the international market (Tab. ~~??~~ S1, in the supplement, lists a few examples with some basic specifications). Besides the attractive low cost, most of these sensors are ~~light~~ also lightweight and have low power requirements. However, as shown in Tab. ~~??~~S1, the errors reported by their manufacturers are larger than what might be measured as the maximum concentration variation when performing an atmospheric vertical profile. To mitigate this accuracy issue, some researchers investigated methods to characterize and correct them in post-processing (Ashraf et al., 2018; Martin et al., 2017; Gaynullin et al., 2016; Yasuda et al., 2012; Mizoguchi and Ohtani, 2005). In some cases, accuracy was improved from ± 30 ppm to ± 1.9 ppm (Martin et al., 2017). However, according to Kunz et al. (2018), the improvements achieved by Martin et al. (2017); Piedrahita et al. (2014); Yasuda et al. (2012); Mizoguchi and Ohtani (2005) are not applicable to UAS-based sampling due to the stronger rates of change in pressure, temperature, and relative humidity associated

with ~~UAS profiles~~UAS-based atmospheric profiles. Recent publications, such as Arzoumanian et al. (2019), partially address these concerns by increasing the variation range of the test variables. However, these newer results may also not be valid for UAS-based applications due to their longer time scales. Results from Arzoumanian et al. (2019); Martin et al. (2017); Piedrahita et al. (201 were obtained for experiments done in months, weeks, and days. The changes in pressure, temperature, and relative humidity associated with UAS atmospheric profiles occur in the time scales of minutes.

~~Another issue that arises when using~~ In their work, Martin et al. (2017) present a comparison between a sequential method to correct the impacts of pressure, temperature, and humidity versus a joint correction method using multivariate linear regression. This provides some insight into the impact of each variable on low-cost ~~NDIR-based~~ NDIR CO_2 sensors~~for atmospheric measurements is their uncertain sample diffusion time. None of the~~. However, important questions for UAS-based measurements remain unanswered. For example, is the 0.1 ppm improvement in RMSE for temperature corrections (sequential method) a factor of the small impact of temperature on NDIR CO_2 sensors or a factor of the small range of temperatures tested? Was the impact of temperature obfuscated by the larger impact of pressure? Even though a realistic method to mitigate the impact of environmental variables on low-cost NDIR CO_2 sensors ~~available in the market was designed~~ for UAS-based ~~deployment. Therefore, their optical chambers assume a natural air exchange with the environment over a long period (minutes to hours). This design characteristic creates an artificially slow time response. To mitigate this issue, some manufactures offer optional airflow intakes for the sensors~~ measurements should account for the joint variation of pressure, temperature, and relative humidity, understanding the isolated behavior of each variable is important to inform the design of UAS-based sensor packages. This knowledge can help system developers address some of these measurement issues during the sensor package design phase (e.g., ~~CO2Meter's pump cap for the K30), and some researchers design custom sensor housings to control airflow and integrate the sensors into the aircraft~~ heat shielding), thus reducing issues to be corrected in post-processing. ~~These custom sensor housings, such as the one designed by B. H. de Azevedo (2020), can improve the sensor time response from 30 to approximately 1 (under 0.5 flow). However, it is important to note that spatiotemporal results from systems using this technique are averaged and assume some degree of spatiotemporal homogeneity. Therefore, their use in some plume tracking applications, amongst others, is limited~~

Another motivation for isolating the impacts of each of these three variables is the study of the impact of relative humidity. Many low-cost systems for atmospheric CO_2 measurements rely on desiccants to eliminate errors induced by variations in relative humidity. Therefore, there are few correction methods for this variable in the literature. Understanding the impact of this variable is crucial for UAS-based applications due to the design impacts in aircraft size, weight, and power, from the addition of a desiccant compartment. Desiccants need to be replaced periodically. Thus, their placement choice on the aircraft is limited by their accessibility requirement. Furthermore, a desiccant container creates an additional air-volume in the measurement system, which can impact the spatiotemporal resolution of UAS-based systems. Finally, using of desiccants in UAS-based applications implies on the use of pumps to actively control the system's airflow. The use of pumps increases the total system weight and power requirements when compared to ram-air solutions.

Finally, any system used to support long-term research or forecast operations should also account for temporal drift and sensor decay. In the case of UAS-based applications, this decay may happen in short periods due to the intense exposure to the

elements and the amount of dust collected during aircraft take-off and landing. Sensor decay periods vary with application and require a case-by-case length determination. Therefore, another concern regarding the adoption of the correction methods currently available in the literature is their complexity. Most of the correction methods for low-cost NDIR CO_2 sensors available in the literature rely on periodic recalibration using a traceable gas canister. These can be done either through complex laboratory setups or day-long field calibrations using ambient pressure and temperature variations. Although there is no question that traceable gas canisters provide the most precise means of calibration and correction, this method is not practical for UAS-based field applications. Certainly, a UAS-based measurement system can be calibrated in a laboratory before and after a field campaign. Nevertheless, for field operations involving multiple flights per day over multiple days, a low-complexity method using a reference gas analyzer may be beneficial for field calibrations.

~~As mentioned previously, changes in~~ In this study, we attempt to address some of the abovementioned concerns. First, we test a low-complexity method using a reference gas analyzer on a chamber setup to study the isolated impacts of pressure, temperature, and ~~humidity can interfere with NDIR sensors. Even though some studies have addressed~~ relative humidity on low-cost NDIR CO_2 sensors. Then, we evaluate a low-cost benchtop setup to characterize and correct the impact of ~~environmental variables on these sensors, they have done so through lumped correction methods (e. g. , multivariate linear regression analysis in Martin et al., 2017). These lumped approaches limit the understanding of the individual impact of each variable, and are not robust for wide variation ranges. These limitations may prevent system developers from addressing measurement requirements during the sensor package design phase~~ these variables on the same sensors. For all of these experiments, we attempt to increase the test range for each variable and reduce the experiment time scales. More details on each experiment and their results are shown in sections 2, 3, and 4.

2 Methodology

As mentioned previously, the strong rates of changes in pressure (P), temperature (T), and relative humidity (RH) associated with UAS-based atmospheric measurements can interfere with low-cost NDIR CO_2 sensors. For a given test variable, these rates of change are determined by the number of units changed per time interval (e.g., ~~heat shielding),thus creating more issues to be corrected in post-processing. To address this limitation, we increased the experimental conditions of the previous characterization procedures~~ $\Delta P/\Delta t$, $\Delta T/\Delta t$, and $\Delta RH/\Delta t$, where t is the time). In this study we are interested in variations between 10 and 45 °C, 5 and 95 %RH, and 60,000 and 101,325 Pa[2] that occur in time intervals from 10 to 120 minutes. We have chosen these intervals based on the performance limitations of most of the commercially available low-cost UAS and the sampling pattern recommendations for UAS-based measurements found in the literature ~~to adequate them to UAS flight conditions. We also isolated the effects of~~ (Houston and Keeler, 2018; Hemingway et al., 2017). We are aware there is interest in UAS-based sampling of atmospheric CO_2 outside of these intervals. However, as they may fall outside the capabilities of low-cost NDIR CO_2 sensors and low-cost UAS, they are not the focus of this study.

[2]This pressure interval may seem large for low-cost commercially available UAS. However, these pressures are commonly experienced for UAS flights at elevated locations. For example, flights near Boulder, Colorado (Barbieri et al., 2019)

Besides the desire to characterize and mitigate the impact of pressure, temperature, and relative humidity on ~~an NDIR sensor and analyzed their impact separately. More information about the experiments is given in sections ?? through 4.0.1.~~ low-cost NDIR CO_2 sensors, this study is also focused on performing this task via a low-complexity method that would be accessible to a larger portion of the scientific community. Therefore, the experiments in this study were performed via comparison to a calibrated reference gas analyzer. This strategy eliminates the need for traceable gas canisters and their plumbing and chamber-sealing requirements while increasing the number of potential instruments to produce the desired changes in pressure, temperature, and relative humidity. Nonetheless, it is important to note that this strategy is limited to producing results relative to the reference gas analyzer. It is also important to note that the selected reference gas analyzer must be independent of changes in the test variables within the test range. More details about this requirement and other limitations of this method can be found in sections 2.1, 3, and 4.

3 ~~Methodology~~

The experiments in this article were organized into two parts. The first part is a collection of experiments done in the environmental chambers of the Oklahoma Mesonet's calibration laboratory. These experiments provide a baseline of the impact of each variable on low-cost NDIR CO_2 sensors and an initial evaluation of the correction methods based on a reference gas analyzer. The second part is a collection of low-cost benchtop experiments performed to evaluate if a method using a reference gas analyzer and limited resources can be developed for field calibrations. A complete list of experiments can be found on Tab. S3 (see supplement). The following subsections detail the selection process of the low-cost NDIR CO_2 test sensors and the characteristics of the selected reference sensors.

2.1 Test Sensors

Due to the large number of low-cost NDIR-based CO_2 sensors available and the unfeasibility of evaluating all of them, we searched the literature for model comparison studies and the rate of adoption of each model. We used this methodology to select a model that would represent the current state of the art for low-cost UAS-based atmospheric CO_2 sampling. In a comparison study, Yasuda et al. (2012) evaluated five different models and concluded that the Senseair K30 NDIR CO_2 sensor offered the best combination of cost, weight, and accuracy ~~between~~ among the models considered. A similar result was found by Al-Hajjaji et al. (2017), who compared five other sensors to the K30.

The adoption of the K30 for UAS-based measurements was compared to the adoption of other models by their use in the reviewed literature~~. The~~, and the adoption of these sensor models in the literature was evaluated through a search on the GoogleScholar™ database. This search followed the method from the literature review on UAS-based gas sampling ~~done~~ by Villa et al. (2016). The list of search terms and resulting analysis can be found in Tab. ??S2. The analysis suggests that the K30 is more prevalent in the literature than the other models tested by Yasuda et al. (2012) and Al-Hajjaji et al. (2017). For these reasons, all experiments in this article were performed with the Senseair K30 NDIR CO_2 sensor.

To evaluate the individual impact of pressure, temperature, and humidity on Neither the Senseair K30 nor the other low-cost NDIR sensors, we performed two sets of experiments. The first set was performed at the Oklahoma Mesonet Calibration Laboratory to explore each variable's impact at more extensive variation ranges. The environmental chambers of the Oklahoma Mesonet Calibration Laboratory allow great control over each variable, creating appropriate conditions to simulate UAS flights. A description of CO_2 sensors evaluated by Yasuda et al. (2012) and Al-Hajjaji et al. (2017) were designed for UAS-based deployment. Their optical chambers assume a natural air exchange with the environment over a long period (minutes to hours). This design characteristic creates an artificially slow time-response. To mitigate this issue, some manufacturers offer optional airflow intakes for the sensors (e.g., CO2Meter's pump cap for the K30), and some researchers design custom sensor housings to control airflow and integrate the sensors into the aircraft. These custom sensor housings, such as the ones shown in B. H. de Azevedo (2020), can improve the sensor time response from 30 s to approximately 1 s (under 0.5 Ls^{-1} flow). However, it is important to note that spatiotemporal results from systems using this technique are averaged and assume some degree of spatiotemporal homogeneity. Furthermore, sensor housings can directly impact the propagation of changes in temperature and relative humidity from the environment to the sensors.

Even though the impacts of sensor housing design are not within the scope of this study, the evaluation of a method to mitigate environmental variables on UAS-based measurements that did not consider the requirements of UAS-based sensor deployment would not be complete. For this reason, we collocated test sensors in different housing configurations whenever the chamber space allowed for. In total, we used three housing configurations. The first housing configuration is a simple box of approximately 200 mL that houses two K30 units and an IST HYT-271[3] temperature and humidity sensor. The second configuration is similar to the Oklahoma Mesonet and its facilities can be found in McPherson et al. (2007). The second set of experiments was performed on a regular laboratory workbench. These experiments were designed to expand the results from the first set of experiments and evaluate the feasibility of deriving correction coefficients from low-cost experimentsfirst but has its volume reduced to only expose the optical chambers of the two K30 and the HYT-271 sensor to the controlled airflow. Its volume is approximately 8 mL. Both configurations use a 0.5 Ls^{-1} diaphragm pump to control the airflow in and out of the housing. Details for each experiment and results are given in sections ?? through 4.0.1. the shape and design of both sensor housings can be found in B. H. de Azevedo (2020). The third and final configuration has two exposed K30 sensors without any sensor housing, and it serves as a control.

All experiments in this article were performed using two units of the Senseair K30-FR NDIR CO_2 sensor under 0.5 airflow. This strategy was adopted to increase the confidence in the results obtained and evaluate considerations found in the literature regarding the need for distinct correction coefficients for each sensor unit. Finally, it is important to note that all results and analyses in this article considered only the CO_2 concentration values reported by each sensor unit. In other words, each unit was assumed to be immutable from its factory-performed calibration. Therefore, no attempts were made to analyze and correct the light absorption signals within the K30. Instead, each sensor unit was evaluated and corrected as a "black-box". This method was adopted to evaluate if these sensors could produce satisfactory results only with post-processing techniques.

[3] https://www.ist-ag.com/en/products/humidity-module-hyt-271-pluggable-sil-contacts

3 ~~Temperature dependence~~

2.1 Reference Sensors

The ~~temperature dependence experiment performed~~ reference gas analyzers used in this study were the LI-COR LI-840A and LI-820. These gas analyzers served as a control for the experiments because they are also light-based sensors, but they use sample conditioning and auxiliary sensors to eliminate interference from pressure, temperature, and humidity. Both sensors heat the sampled air to 50 °C before measuring its CO_2 concentration. Therefore, the temperature variations tested in this study do not affect their measurements. Both sensors measure the pressure inside their optical chambers and use algorithms for active compensation. However, only the LI-840A measures H_20 (mmol/mol) for algorithmic compensation. For this reason, the LI-840A was used as the comparison reference, placed inside the test volumes with the test sensors (when the designed experiment allowed for it), and the LI-820 monitored the ambient near the experiment for potential variations in the experimental conditions.

Monitoring the ambient conditions near the experiments is important for this comparative study because the unsealed chambers and benchtop setups used can be affected by external increases in CO_2. These chambers and benchtop-setups take ambient air and condition it to create the desired test conditions (e.g., heating the air). Due to this experimental limitation, we reduced external sources of CO_2 and monitored the ambient conditions near the test chambers to ensure that pressure, temperature, relative humidity, and CO_2 did not change significantly during the experiments. This article's supplement shows the ambient conditions for all experiments in this study and two comparison experiments between the test and reference sensors (see Fig. S4). More details on specific experimental setups are given in sections 3 and 4.

3 Chamber Experiments

To investigate the impact of pressure, temperature, and relative humidity on low-cost NDIR CO_2 sensors and evaluate the correction method based on a reference gas analyzer, we performed five chambered experiments at the Oklahoma Mesonet Calibration Laboratory~~used~~. The environmental chambers of the Oklahoma Mesonet Calibration Laboratory are not specialized for gas experiments and present many similarities to other environmental chambers found in other universities and research laboratories. The two chambers used for these experiments were the Thunder Scientific 2500 ~~chamber to produce a temperature variation from 10~~and the Cincinnati Sub-Zero Z16. This particular Z16 was outfitted with a custom gasket-based vacuum and compression system, developed by the laboratory's manager, David L. Grimsley. A description of the Oklahoma Mesonet and its facilities can be found in McPherson et al. (2007).

3.1 Pressure

The pressure dependence experiment performed at the Oklahoma Mesonet Calibration Laboratory used the Cincinnati Sub-Zero Z16 chamber and its custom gasket-based vacuum and compression system. This system produced a pressure variation from 105,000 to 60,000 Pa, in 1,000 ~~to 40 , in ten-degree~~ Pa increments, at ~~a constant 50 . Each temperature~~ 25 °C. Each pressure

change was followed by a ~~two-hour~~ two-minute dwell period. Even though the Cincinnati Sub-Zero Z16 chamber can control temperature and humidity~~are controlled, this chamber is not entirely isolated from the external environment. This means the experiment was executed at the atmospheric pressure conditions for the day in Oklahoma, and the~~ , its controlled conditions are not reflected inside the custom pressure system. This occurs because the Thompson vacuum and compression pumps on the Mesonet's custom pressure system use air from outside the controlled chamber. Therefore, in this experiment, the temperature control is limited to the impacts caused by keeping the entire Mesonet custom pressure system at the chamber's temperature. This setup also does not allow for any active control of relative humidity. This characteristic also means that changes in CO_2 concentration ~~in the laboratory~~ near the chamber could affect the experiment. ~~To mitigate contamination, access to the laboratory was limited during the experiment, but not interrupted. To corroborate the results and evaluate possible contamination,reference gas analyzers were placed inside and outside the chamber. Fig. 4 illustrates the sensor arrangement for this experiment.~~ This type of contamination can create effects that obfuscate the effects of pressure. To mitigate this problem, we reduced the experiment's duration to the pressure system's limits and used the LI-840A to monitor potential contaminations and validate the experimental conditions.

Although the LI-840A pressure compensation range is specified within 15,000 and 115,000 Pa, we chose not to connect this reference sensor to the pressure system based on a consultation with an LI-COR engineer. In this consultation, we were informed that the compensation algorithm could fail for large pressure changes in short intervals. To avoid any problems, the reference sensor was placed adjacent to the intake and exhaust nozzles of the vacuum and compression pumps (as shown in Fig. 1). This placement still allowed us to monitor the parameters of the air used by the pressure system to produce the changes on the test sensor. The metrics for the experimental conditions can be seen on Tab. S10. In this experiment, it was only possible to deploy the K30 sensors using the first housing configuration (200 mL box, see section 2.1 for more details). This limitation was created by the connection requirements of the Mesonet custom pressure system.

~~The reference gas analyzer inside the chamber was~~ As can be seen on Tab. S10, the ~~LI-COR LI-840A.This sensor served as a control because LI-840A is also a light-based sensor, but it uses sample conditioning to eliminate interference from pressure, temperature, and humidity. The LI-840A heats the sampled air to 60~~HYT-271 sensor inside the K30 sensor housing reported standard deviations of 0.98 %RH for relative humidity and 0.03 °C ~~before measuring its CO_2 concentration. Therefore, the variation from 10~~for temperature. This indicates that the majority of the 230 ~~to 40 inside the chamber does not affect its measurements. The gas analyzer outside the chamber was the LI-COR LI-820. This analyzer served as a reference for the experiment conditions within the laboratory. For these reasons, in this article, the LI-840A and the LI-820 are referred to as independent sensor (inside) and independent sensor (outside), respectively.~~

~~The results for the Mesonet temperature dependence experiment are shown here in two formats. The first format, in Fig. **??**, shows the time series for the chamber's temperature and the reported concentrations for all four CO_2 sensors. The second format,~~ ppm change, seen in Fig. ~~**??**, shows the scatter plots and correlation coefficients for all six comparisons between the test sensors , test variable, and reference sensors.~~ 2, in both test sensors was caused by the 45,000 Pa change in pressure. This result is impressive considering that the air used by the pumps to produce these pressures showed only a 2.55 ppm standard deviation for CO_2 during the same period.

~~Experiment diagram for temperature and relative humidity at the Oklahoma Mesonet Calibration Laboratory. Two test sensors were placed inside the chamber with a control sensor, and a reference sensor was placed outside to detect possible contamination.~~

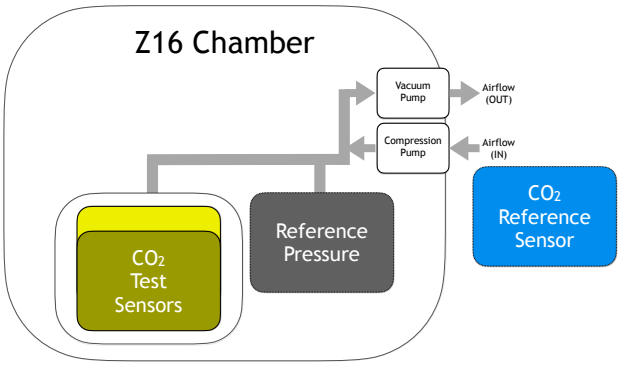

Figure 1. Diagram for the Pressure Chamber Experiment. Two test sensors were placed inside the chamber, and a reference sensor was placed outside to indicate possible contamination and monitor the experimental conditions.

~~Time-series data for the Mesonet temperature dependence experiment. The solid black curve represents the temperature inside the chamber. The orange curves represent the CO_2 concentrations reported by the independent and test sensors. The black (left) and orange (right) y-axes provide the scales for temperature and CO_2 measurements, respectively.~~

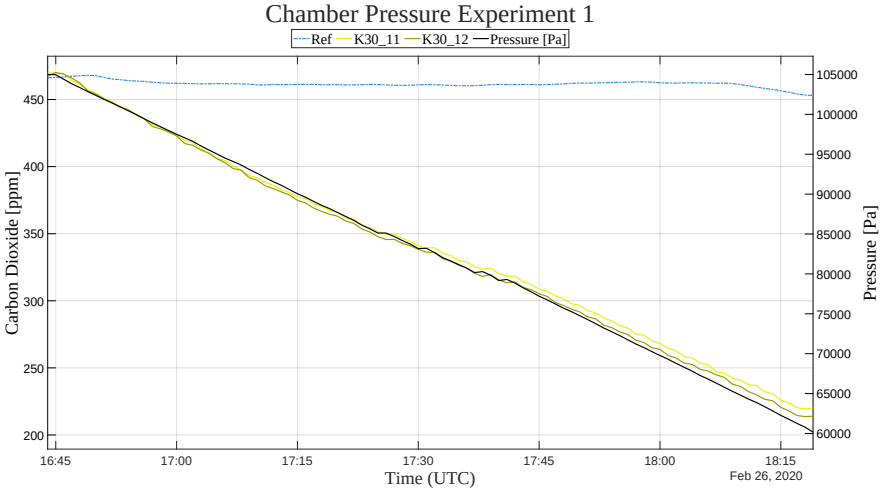

Figure 2. Time-series data for the Pressure Chamber Experiment. The solid black curve represents the pressure inside the chamber. The yellow curves represent the CO_2 values reported by the test sensors. The dashed blue curve represents the CO_2 values reported by the reference sensor.

3.1.1 CO_2 Pressure Correction

Analyzing the time-series data for the experiment, there only seems to be an increase in COWithin the NDIR sensor literature, the article by Gaynullin et al. (2016) offers an excellent description of the determination of the pressure correction coefficients for the Senseair K30 NDIR CO_2 sensor. According to the authors, the CO_2 when the temperature increases from 20 to 30concentration reported by the sensors can be corrected by the following equation,

$$PPM_{corrected} = \frac{PPM_{measured}}{k_1 * (P - P_0)^3 + k_2 * (P - P_0)^2 + k_3 * (P - P_0) + k_4}, \quad (1)$$

where the coefficients k_1 through k_4 need to be determined for each sensor unit, and P_0 is 101,325 and from 30Pa. In their article, Gaynullin et al. (2016) report a maximum deviation between the corrected and true value between 2 and 4 to 40 . However, this CO_2 increase is also observed more than one hour after each temperature change, during the dwell periods for 30 and 40 . Furthermore, similar CO_2 increases are also observed on the internal and external independent sensors. This leads us to believe the experiment was contaminated by an increase in concentration in the laboratory. This hypothesis is supported by the stronger correlations between the test sensors and the independent sensors than the correlations between the test sensors and temperature.

Scatter plots and correlation coefficients for the Mesonet temperature dependence experiments. The first row shows the correlations for Test Sensor 1. The second row shows the correlations for Test Sensor 2. The first column shows the correlations with temperature, the second column with the Independent Sensor (inside), and the third column with the Independent Sensor (outside).

Further analyzing the correlation between temperature and the test sensors, we note a change in behavior around the 16:51 timestamp. Before this timestamp, the correlation coefficient between temperature and test sensors was −0.18 (for sensor 1) and 0.04 (for sensor 2). After this timestamp, both coefficients increase (0.86 and 0.92, respectively). This increase coincides with the sudden increase in the reported concentration outside the test chamber. We cannot find evidence to support temperature dependence when evaluating the temperature correlation coefficients during the temperature changes (summarized in ppm. However, their results were obtained using a complex multilayered chamber that pressurized a reference gas. Unfortunately, such an experimental setup is not practical for low-cost UAS-based applications. In this section, we evaluate the feasibility of determining the pressure correction coefficients using the CO_2 values measured by the reference gas analyzer. We assume the low variability in pressure, temperature, and humidity found in a short-duration experiment mimics the controlled conditions found in Gaynullin et al. (2016). Our results for this first evaluation can be found in Fig. 3 and Tab. ??)1.

To rule out any minor temperature dependence effects obscured by the interference on the Mesonet experiment,a second experiment was performed focused on the temperature change from 20 Over the span of 45,000 Pa, the maximum absolute errors (MxAE) reported by the test sensors were 8.7 and 8 ppm, and the root mean squared errors (RMSE) were 2.15 and 1.91 ppm. These are considerable improvements over the original 233.9 and 239.65 MxAE and the 140.09 and 143.75 RMSE. Nonetheless, it is important to highlight that these results are not absolute. They are relative to the values reported by the

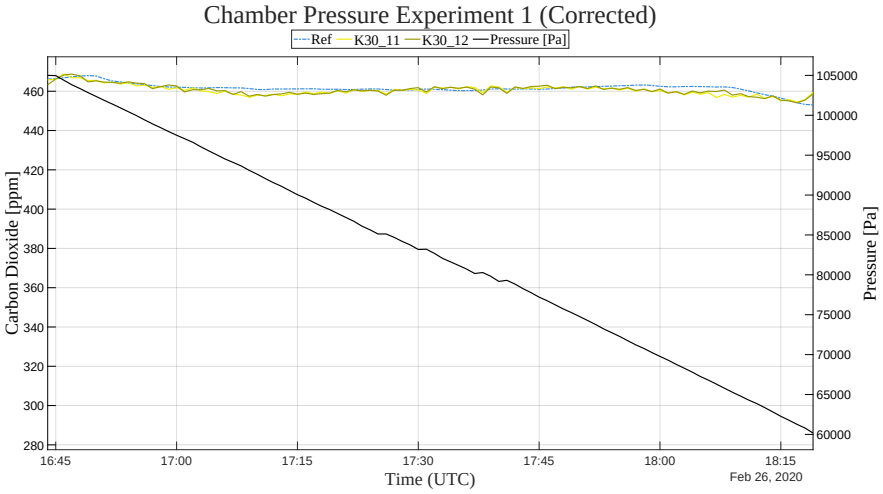

Figure 3. Time-series data for the Pressure Chamber Experiment after the application of the correction method. The solid black curve represents the pressure inside the chamber. The yellow curves represent the CO_2 values reported by the test sensors. The dashed blue curve represents the CO_2 values reported by the reference sensor.

Table 1. ~~CO_2 correlation coefficient~~ Coefficients from the pressure correction method and root mean square errors for ~~each~~ the test sensors relative to the reference sensor, ~~for each temperature change, during~~ before and after the ~~Mesonet temperature dependence experiment~~correction.

~~Temperature C~~Sensor	k_1 * ~~Sensor 1~~	k_2 *	k_3 *	k_4 *	R^2 *	RMSE ~~Sensor 2~~Before
~~From 10 to 20~~K30_11	~~-0.97~~-2.3291e-16	~~-0.80~~**From 20 to 30**4.1525e-12	~~-0.81~~1.2380e-05	~~0.64~~1.0648	0.9995	140.09
~~From 30 to 40~~K30_12	~~0.58~~-3.4693e-16	~~0.97~~2.8776e-12	1.2778e-05	1.0706	0.9996	143.75

reference gas analyzer. Unfortunately, the test sensors were damaged after this experiment and a second validation run was not possible. However, the results for four other cases using this method on the low-cost bench setup are reported in section 4.1.

3.2 Temperature

The temperature dependence experiment performed at the Oklahoma Mesonet Calibration Laboratory used the Thunder Scientific 2500 chamber to produce a temperature variation from 10 to 40 °C. ~~This second experiment was performed as a low-cost benchtop experiment, with the two test sensors and~~ , in ten-degree increments, at a constant 45 %RH. In this experiment, the ~~LI-840A (Fig. **??**) . In this experiment, all three sensors were allowed to stabilize to outdoor pressure, temperature, and humidity~~

~~conditions (97631.40~~temperature is slowly raised from 10 to 40 ~~, 21.85~~°C in approximately 210-minutes, then reduced back to 10 °C ~~, and 50), then a hot air source emulated a 40 impulse.~~

~~In this second experiment, relative humidity was not controlled as the temperature increased. This uncontrolled method is similar to other experiments found in the literature. The experiment was performed as quickly as possible to avoid contamination due to human exhalation~~in approximately 90-minutes. he operational limits of the chamber defined these time intervals. Nonetheless, this experiment setup allows us to acquire many samples for each temperature and produces conditions that match UAS flight conditions in the final 90-minutes.

The Thunder Scientific 2500 chamber uses a three-chamber system where air from the laboratory is taken and conditioned to the desired set points in the first two inner chambers and then inserted into the test chamber. Besides the ~~experiment speed, the laboratory windows were opened, and a large fan was used to bring outside air into the laboratory constantly. A small mixing fan was also placed near the three sensors (~~potential for external interference through the chamber's air intake, the chamber's test volume also has a cable port that is only partially closed. To counter this external potential external interference, the chamber constantly corrects small changes in temperature and relative humidity, but it offers no control over pressure. For our experiments, besides any pressure-induced changes in the reported CO_2, actual concentration changes in the laboratory taken in by the chamber can also obfuscate the impacts of the test variables. To mitigate potential contamination, we reduced the experiment's duration to the chamber's operational limits and performed our experiments overnight when there were no people in the laboratory. To validate the experimental conditions, we adopted a strategy similar to the one used for the pressure experiment. However, in this case, the LI-840A reference sensor (Ref) was colocated with the test sensors inside the chamber, and the LI-820 (Ref_Lab) was placed near the chamber's air intake to monitor the experimental conditions. Fig. ~~??)~~4 illustrates this sensor arrangement.

~~The benchtop experiment's time-series data and their corresponding scatter plots are shown in Figs. ?? and ??. In this experiment, the absence of temperature dependence is evident. Even though there is a slight 10~~In this experiment, we used six K30 test sensors, organized in three pairs, following the three sensor housing configurations detailed in section 2.1. The sensors labeled K30_13 and _14 (Test System 1) are in the third configuration (without sensor housing) and serve as a control. As can be seen on Tab. S11, the HYT-271 sensors inside the K30 sensor housings for Test Systems 2 and 3 reported standard deviations of 1.3 and 1.51 %RH. The pressure sensors for all three test systems reported an average standard deviation of 135 ~~increase in the reported concentration of~~ Pa. During the same period, the ~~test sensors, it occurs a full minute after the temperature is brought back near its original state. This same increase is simultaneously seen on the independent sensor, indicating the increase~~ reference sensor inside the chamber showed a 4.02 ppm standard deviation for CO_2. This leads us to believe that the majority of the 36 ppm change seen in five of the six test sensors (Fig. 5) was caused by ~~an external factor. This conclusion is supported by the weak correlation to temperatureand the strong correlation to the independent sensor~~the 30 °C change in temperature.

~~Correlation coefficients for the benchtop temperature dependence experiment. The results are presented as a matrix. The first row shows the correlations for Test Sensor 1. The second row shows the correlations for Test Sensor 2. The first column shows the correlations with temperature, and the second column with the Independent Sensor (inside).~~

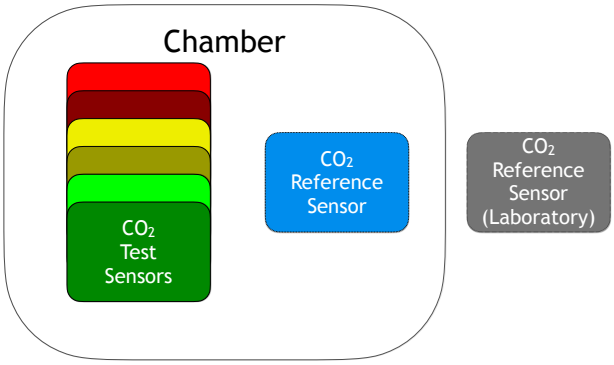

Figure 4. Diagram for the ~~benchtop~~ sensor placement during the temperature and relative humidity experiments at the Oklahoma Mesonet Calibration Laboratory. ~~All~~ Six test sensors ~~are stabilized to~~ were placed inside the ~~environment~~chamber with a reference sensor, ~~then exposed to the heat~~ and ~~humidity source, and finally brought back~~ another reference sensor was placed outside to ~~the environmental conditions by the large mixing fan~~detect possible contamination.

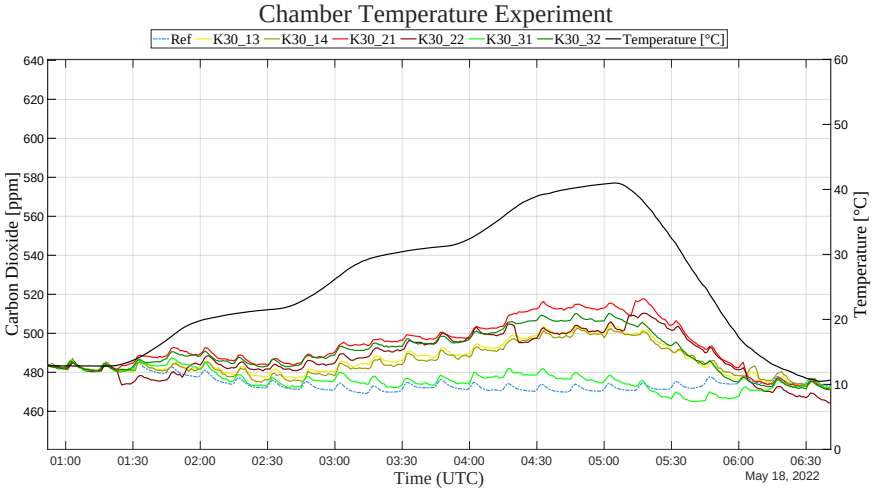

Figure 5. ~~Time series~~ Time-series data for the ~~benchtop~~ chambered temperature ~~dependence~~ experiment. The solid black curve represents the temperature ~~near~~ inside the ~~sensors~~chamber. The ~~three orange~~ yellow, green, and red curves represent the CO_2 ~~concentrations~~ values reported by the ~~independent and~~ test sensors. The ~~black (left) and orange (right) y-axes provide~~ dashed blue curve represents the ~~scales for temperature and~~ CO_2 ~~, respectively~~values reported by the reference sensor.

3.2.1 CO_2 Temperature Correction

4 ~~Relative Humidity Dependence~~

~~The relative humidity (RH) dependence experiment performed at the Oklahoma Mesonet Calibration Laboratory was executed under the same experiment setup detailed in section ?? and illustrated by Fig. 4. In this experiment, the chamber produced an RH variation from 15~~Many of the authors cited in section 1.1 employ a linear regression to correct the impacts of temperature on low-cost NDIR CO_2 sensors. However, the fast reduction from 40 to. 10 °C in our experiments produced some variations in the CO_2 values reported by the test sensors that were better captured by a cubic fitting (similar to the one presented in section 3.1.1, with $T_0 = 15$ ~~to95 at a constant 25 °C. A one-hour dwell period followed each RH level change. The results for the Mesonet RH dependence experiment are shown here in two formats.The first format, in Fig. ??, shows the time-series data for the chamber's RH and the reported concentrations for all four CO_2 sensors.The second result format, in Fig. ??, shows~~). This cubic-like behavior could be a function of small variations in the other variables (e.g., pressure and CO_2), given that our simplified setup does not actively control them. However, the ~~scatter plots and correlation coefficients for all six comparisons between the test sensors, test variable, and reference~~ small scale of the variations in pressure and CO_2 during the experiment lead us to suspect other sources (e.g., a temperature time response effect). Unfortunately, our experimental setup does not allow us to investigate this variation further. Table 2 shows the coefficients and the R-squared for the fitting, and the RMSE relative to the reference sensor, before and after the correction. Figure 6 shows the time series for the corrected test sensors.

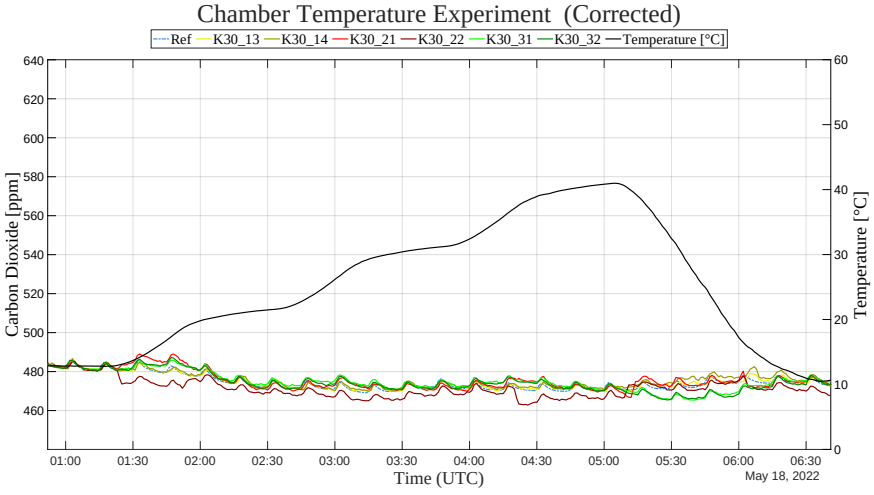

Figure 6. Time-series data for the ~~Mesonet relative humidity dependence~~ chambered temperature experiment after the application of the correction method. The solid black curve represents the ~~relative humidity~~ temperature inside the chamber. The ~~orange~~ yellow, green, and red curves represent the CO_2 ~~concentrations~~ values reported by the ~~independent and~~ test sensors. The ~~black (left) and orange (right) y-axes provide~~ dashed blue curve represents the ~~RH and~~ CO_2 ~~scales, respectively~~values reported by the reference sensor.

Table 2. ~~Scatter plots and correlation coefficients~~ Coefficients for the ~~Mesonet relative humidity dependence experiment~~temperature correction method. The ~~first row shows the correlations for Test Sensor 1. The second row shows the correlations for Test Sensor 2. The first column shows the correlations with~~ RMSE values are relative ~~humidity, to~~ the ~~second column with the Independent Sensor (~~reference sensor inside ~~), and~~ the ~~third column with the Independent Sensor (outside)~~test volume.

Sensor	k_1	k_2	k_3	k_4	R^2	RMSE			
*	*	*	*	*	*	Learn		Test	
						Before	After	Before	After
K30_13	-2.7197e-06	0.0002	0.0023	1.0814	0.9873	15.77	1.12	-	-
K30_14	-2.3352e-06	0.0002	0.0018	1.1381	0.9738	14.83	1.69	-	-
K30_21	6.6562e-07	2.1862e-05	0.0048	0.8204	0.9823	23.99	2.38	20.84	4.09
K30_22	-5.9848e-06	0.0002	0.0043	1.0170	0.9887	19.26	3.91	19.28	3.25
K30_31	2.0487e-07	-1.4397	0.0008	1.2151	0.2949	4.3	2.99	5.87	4.79
K30_32	-7.8179e-07	6.3524e-05	0.0038	0.8544	0.9554	20.24	2.88	17.96	2.88

~~Initial analysis of the experiment's results shows a high correlation coefficient between RH and both test sensors. The results also show an increase in CO_2 when relative humidity is at or above 75 .This same behavior is observed when the correlation coefficients are calculated for each RH transition period (summarized in Tab. **??**). Further analyzing the results, we note the increase in reported CO_2 concentration continues during the entire dwell period for the 75, 85, and 95 levels~~After we determined the coefficients for each sensor, we also used them to correct the data obtained by another run of the same experiment (a test run). This independent test allows us to better evaluate the method's performance. The plots and tables with the data for the test run of the chambered temperature experiment can be found in this article's supplement (S11 through S14). The RMSE for the test run can be found here in Tab.2. These two experiments demonstrate satisfactory error reductions for all sensors except for K30_31. This sensor did not seem to respond to temperature in the same manner as the other five test sensors. Evaluating the behavior of the K30_32, which was placed in the same sensor housing as the K30_31 and behaved similarly to all other sensors, we can eliminate any housing-induced effects. Furthermore, ~~similar CO_2 increases were also observed on the internal and external independent sensors. This leads us to believe the experiment was again contaminated by an increase in concentration in the laboratory. This hypothesis is supported by a stronger correlation between the test and independent sensors.~~ the temperature and relative humidity recorded by this test system's internal HYT-271 followed the chamber's state. Therefore, we have to consider the K30_31 as an outlier for these experiments.

~~To rule out any minor humidity dependence effects obscured by the interference on the Mesonet experiment , a second experiment was performed focused on the RH changes above 75 . This second experiment was performed in the same setup for the low-cost benchtop experiment~~

3.1 Relative Humidity

The chambered relative humidity experiment was also performed on the Thunder Scientific 2500 chamber with the same sensor arrangement described in section ~~?? and illustrated by Fig. ??. The only difference was the substitution of the heat impulse source for a humidity source.~~ 3.2. The two runs for this relative humidity experiment were performed immediately after each temperature experiment run. This strategy allowed us to use the contamination mitigation techniques in a stable laboratory environment. In this experiment, ~~all three sensors were allowed to stabilize to outdoor pressure, temperature, and humidity conditions (97644.02 , 23.46~~the chamber produced a relative humidity (RH) variation from 15 to 85 %RH at a constant 25 °C~~, and 48.08~~. In the first 75 minutes, the RH was raised from 15 to 85 %RH ~~), then a source of humid air emulated a 65~~and then reduced back to 15 %RH ~~step, followed by an 80 step.~~

~~The benchtop experiment's time series and the correlation coefficients are shown Fig. ?? and ??. In~~ over a 13 minutes interval. Again, these time intervals were defined based on the chamber's operational limitations. For the duration of this experiment, the ~~absence of humidity dependence is evident. Even though there is a 4~~HYT-271 sensors inside the K30 sensor housings for Test Systems 2 and 3 reported standard deviations of 0.43 and 0.31 °C for temperature, and all three test systems reported an average standard deviation of 94.5 Pa. This indicates that the average 16 ppm increase ~~in the reported concentration of the test sensors , the same increase is simultaneously seen on the independent sensor. This indicates an external factor may have caused the increase. This conclusion is supported by the weak correlation to humidity and the strong correlation to the independent sensor.~~ across the six test sensors was caused by the 70 %RH change in relative humidity (Fig. 7).

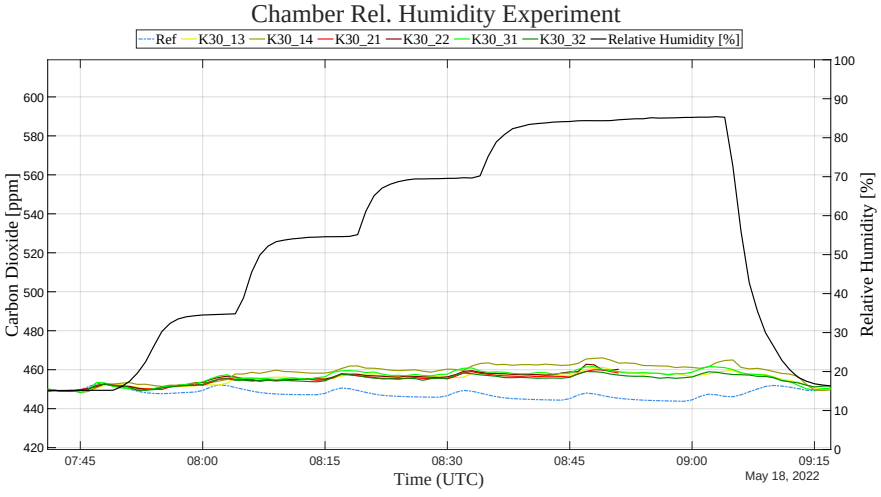

Figure 7. Time-series data for the chambered relative humidity experiment. The solid black curve represents the relative humidity inside the chamber. The yellow, green, and red curves represent the CO_2 values reported by the test sensors. The dashed blue curve represents the CO_2 values reported by the reference sensor.

3.1.1 CO_2 Relative Humidity Correction

As mentioned in section 1.1, there are few methods in the literature to correct the impact of humidity on low-cost NDIR CO_2 sensors. Most of the methods found adopt a simple linear regression correction, but for the reasons mentioned in section 3.2.1, we also adopted a cubic fitting (see section 3.1.1) for our correction. In this case, with $RH_0 = 36\%$. We believe the 70 %RH change in 13 minutes is considerably stronger than any other experiments shown in the literature. Thus, more prone to reveal effects not seen before. Table 3 shows each test sensor's coefficients, the R-squared for the cubic fitting, and the RMSE relative to the reference sensor. Figure 8 shows the results of this correction method.

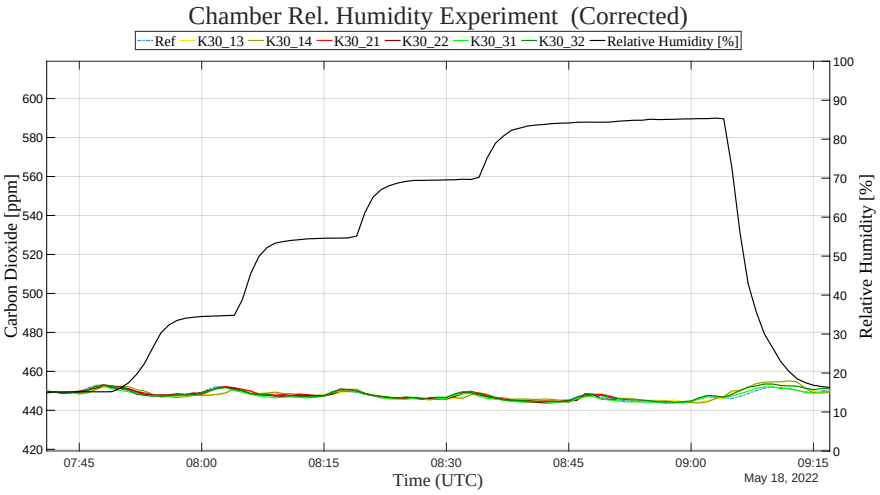

Figure 8. Time-series data for the chambered relative humidity experiment after applying the correction method. The solid black curve represents the relative humidity inside the chamber. The yellow, green, and red curves represent the CO_2 values reported by the test sensors. The dashed blue curve represents the CO_2 values reported by the reference sensor.

~~Time-series data for the benchtop relative humidity dependence experiment. The solid black curve represents the relative humidity inside the chamber. The orange curves represent the CO_2 concentrations reported by the independent and test sensors. The black (left) and orange (right) y-axes provide the relative humidity and CO_2 scales, respectively.~~ To better evaluate the method's performance, we repeated the experiment and applied the previously determined correction coefficients to it. This independent test mimics how the method would be applied to correct field data. The plots and tables with the data for the other chambered relative humidity experiment run, the test run, can be found in this article's supplement (S15 through S17). The RMSE for the test run can be found here in Tab. 3. These two experiments demonstrate satisfactory error reductions for all sensors except for the sensors in Test System 3 (K30_31 and K30_32) during the test run. Further evaluating these results, we noted that the method overcorrected these two sensors on the test run. This overcorrection can be explained by the difference in the range of %RH effectively transferred inside the sensor housing between the two experiments. In the first run of the experiment, when the coefficients were determined ("learn" case), the minimum and maximum %RH inside the housing of

Table 3. ~~CO_2 correlation coefficients for each test sensor, for each RH change, during~~ Coefficients from the ~~Mesonet~~ relative humidity ~~dependence experiment~~correction method. The RMSE values are relative to the reference sensor inside the test volume.

~~RH %~~Sensor *	k_1 ~~Sensor 1~~	k_2 ~~Sensor 2~~	k_3 *	k_4 *	R^2 *	RMSE Learn Before	RMSE Learn After	RMSE Test Before	RMSE Test After
~~From 15 to 35~~K30_13	~~0.05~~8.1074e-08	~~0.23~~-4.6056e-06	0.0008	1.1071	0.9180	9.02	1.31	-	-
~~From 35 to 55~~K30_14	~~0.80~~1.200e-07	~~0.78~~-7.4641e-06	0.0011	1.1559	0.9262	12.37	1.62	-	-
~~From 55 to 65~~K30_21	~~0.96~~2.0367e-07	~~0.91~~-4.5196e-06	0.0009	0.8858	0.9819	8.09	0.66	9.73	2.38
~~From 65 to 75~~K30_22	~~−0.77~~5.2379e-07	~~−0.76~~-2.5196e-06	0.0009	1.0617	0.9848	8.82	0.58	10.91	2.52
~~From 75 to 85~~K30_31	~~0.94~~9.6294e-08	~~0.86~~-5.9337e-06	0.0011	1.2191	0.9864	9.72	0.63	5.36	4.81
~~From 85 to 95~~K30_32	~~0.96~~1.4859e-07	~~0.95~~-4.9691e-06	0.0007	0.9179	0.9681	8.07	0.85	16.14	9.58

TS_3 were 12.15 and 68.8 %RH. During the second run, when the coefficients were tested, the minimum and maximum %RH inside the housing were 14.53 and 74.41 %RH.

~~Scatter plots and correlation coefficients for the benchtop relative humidity dependence experiment. The results are presented as a matrix. The first row shows the correlations for Test Sensor 1. The second row shows the correlations for Test Sensor 2. The first column shows the correlations with relative humidity and the second column with the Independent Sensor (inside).~~ Even though this particular result may point to potentially negative effects of the sensor housings, we highlight that all four housed sensors outperformed the unhoused (control sensors) in the first run (see Tab. 3). Similar errors, caused by slight differences in experimental conditions between the "learn" and "test" cases, were also seen in the development of the benchtop pressure experiments. This error can be mitigated by increasing the number of "learn" cases presented to the coefficient determination algorithm. This strategy creates an averaged set of coefficients for a particular sensor unit that is more robust.

4 ~~Pressure Dependence~~

3.1 Join Correction

~~The pressure dependence experiment performed at the Oklahoma Mesonet Calibration Laboratory used the Cincinnati Sub-Zero Z16 chamber with a custom gasket-based vacuum and compression system. This custom system was developed by the laboratoryâs manager, David L. Grimsley. This system produced a pressure variation from 105, 000 to 60, 000~~In their work, Martin et al. (2017) present a comparison between a sequential and joint method to correct the impacts of pressure, temperature, and humidity. The sequential method corrects each variable independently in a predetermined order, and the joint method uses multivariate linear regression to correct all variables at once. Their results indicate that the joint method was only 0.27 ~~, in 1~~ppm (on average) better than the sequential method. This slight difference between the two methods should allow researchers to choose the method that

is better suited for their experimental setup. For example, in our setup, the pressure experiments were performed in a different chamber than our temperature and relative humidity experiments. Therefore, the correction coefficients were determined based on different datasets. In this section, we offer an example of a hybrid method where the coefficients for temperature and humidity were determined together, and the pressure coefficients were determined separately. We then demonstrate the joint correction of all three variables on a test case.

Even though the pressure correction method was tested on sensors K30_11, ~~000 increments, under controlled temperature and humidity. Each pressure change was followed by a two-minute dwell period. Even though the temperature~~ K30_12, K30_21, and K30_22, in this example, we only present the results for Test System 2, with test sensors K30_21 and ~~humidity can be controlled, this chamber is not entirely isolated from the external environment. As in previous experiments, this means that changes in CO_2 concentration could affect the experiment, and to mitigate contamination, access to the laboratory was limited during the experiment. A reference gas analyzer was placed outside the chamber to detect possible contamination. Fig. 1 illustrates this sensor arrangement.~~ K30_22 because sensors K30_11 and K30_12 were damaged after the chambered pressure experiments (see Sec. 3.1). The pressure correction coefficients were not determined for the other test sensors used in this study because of the Mesonet pressure system's custom connection requirement (see Sec. 3.1), and the benchtop pressure chamber's size limitation (see Sec. 4.1) and radio frequency shielding requirement (see Sec. 5). Therefore, we test our assumption of the equivalence between the sequential and joint methods in Martin et al. (2017) using the pressure correction coefficients determined in section 4.1 and a new cubic fitting of the joint variation of temperature and relative humidity obtained from the data shown in section 3.2. This hybrid set of coefficients requires the data to be corrected for pressure first and then jointly corrected for temperature and relative humidity.

~~Diagram for the Mesonet pressure experiment. Two test sensors were placed inside the chamber and a reference sensor was place outside to indicate possible contamination.~~

~~In this experiment, the LI-840A gas analyzer was not placed inside the chamber because its pressure compensation is not rated for this magnitude of pressure change. Instead, it was kept outside the chamber as a reference for the experiment conditions within the laboratory. This external reference was necessary because the pressure system pumps air from the laboratory to increase the pressure from 60, 000~~The coefficients, R^2, and RMSE for the pressure correction step used here can be seen in section 4.1. This article's supplement shows the ten coefficients for the joint temperature and relative humidity cubic fitting (Tab. S18). The cubic fitting's R^2 for sensors K30_21 and K30_22 were 0.9869 and 0.9855. The dataset for the test of the hybrid method presented changes of 378 Pa~~back to 105, 000, 30.51 .~~

~~This experiment showed an extreme dependence between the CO~~°C, and 34.76 %RH. During the same period, the reference gas analyzer presented a change in CO_2 ~~concentration values reported by the test sensors and pressure. A 50~~of 10.54 ppm~~fluctuation outside the chamber produced a small interference during the experiment. However, considering the 250~~. Table 4 and figure 9 show the results for this test. As mentioned above, this test was performed in a hybrid format. The first step, pressure correction, only accounted for an average improvement in the RMSE relative to the reference sensor of 0.64 ppm. The second step, joint correction of temperature and relative humidity, produced an average improvement in RMSE of 26.76 ppm ~~effect produced by the pressure change, this interference did not change the experiment results (see Fig. **??**). This conclusion is corroborated~~

by the correlation coefficients shown in Fig. ??across both sensors. The final RMSEs of 1.73 and 3.15 ppm support our assumption.

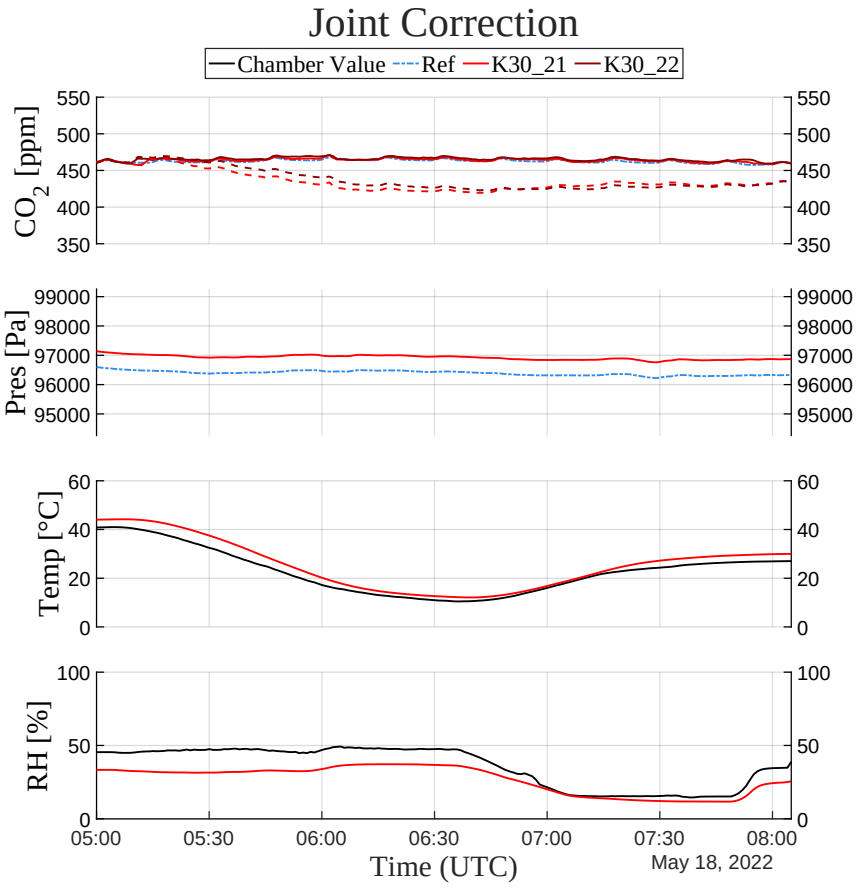

Figure 9. Time-series data for the Mesonet joint correction test for pressuredependence experiment, temperature, and relative humidity. The solid black curve represents the pressure inside experimental conditions for the chambertest. The orange red curves represent the CO_2 concentrations reported by the independent and validation conditions for the test system and its sensors. The black (left) and orange (right) y-axes provide dashed blue curve represents the scales for pressure and CO_2 , respectivelyand validation conditions for the reference sensor.

3.2 CO_2 Pressure correction

4 Benchtop Experiments

Within the NDIR sensor literature, the article by Gaynullin et al. (2016) offers an excellent description of the determination of the pressure correction coefficients for the Senseair K30 NDIR CO_2 sensor. In their article, Gaynullin et al. (2016) indicates

Table 4. ~~Scatter plots and correlation coefficients for~~ Root mean square error relative to the ~~Mesonet pressure dependence experiment~~reference sensor. ~~The first row shows~~ Step 1 represents the ~~correlations for Test Sensor 1. The second row shows the correlations for Test Sensor 2. The first column shows the correlations with~~ pressure correction, and step 2 represents the ~~second column with~~ joint temperature and relative humidity correction after the ~~Independent Sensor (outside)~~pressure correction.

Sensor *	RMSE		
	Original	Step 1	Step 2
K30_21	30.66	30.07	1.73
K30_22	29.02	28.33	3.15

~~that this coefficient determination procedure needs to be performed~~ Many UAS-based atmospheric CO_2 applications involve multiple flights per day over multiple days. In these intense operational periods, the exposure to the elements and the dust collected during take-off and landing may greatly impact sensor decay and temporal drift. Given the uncertainties regarding the decay period for each sensor unit, it is recommended to perform system calibration and correction coefficient determination procedures as often as operationally possible. This recommendation is particularly important for systems supporting long-term research. Unfortunately, most of the procedures available in the literature are not practical for many UAS-based field applications. ~~However, the expertise required to repeat their procedure makes the method inaccessible to most.~~ In this section, we evaluate ~~the feasibility of determining the pressure correction coefficients using a low-cost, readily available vacuum pump and a reference gas analyzer~~a series of low-cost benchtop setups to characterize and correct the impact of pressure, temperature, and relative humidity on low-cost NDIR CO_2 sensors.

4.1 Pressure

The experimental setup for this low-cost procedure (illustrated in Fig. 10) consists of a BACO Engineering 5-Gallon Vacuum Chamber Kit, available at multiple retailers for USD189.99, and the LI-840A gas analyzer. In this setup, the gas analyzer provides the reference ~~concentration~~ CO_2 values for the experiment's initial state. Then, the chamber is closed and isolated from the external environment. Finally, the chamber is depressurized until the top of the emulated ~~UAS-flight~~ UAS flight is reached.

~~Diagram for the benchtop pressure correction experiment. Chamber and sensors stabilize to environment conditions (pre-experiment). Then, the chamber's isolation maintains the initial CO_2 concentration while pressure changes.~~

~~Because this~~ The pressure changes are produced by a microcontroller turning the system's pump "ON" for 2 seconds and then "OFF" for 1.5 minutes. This method uses the ambient CO_2 concentration~~and pressure~~, pressure, temperature, and relative humidity as its initial state~~,~~. Therefore, it also requires the ambient monitoring strategies detailed throughout section 3.

Besides the ambient monitoring strategies, the benchtop version of the coefficient determination method described in section 3.1 also requires multiple runs of the experiment to achieve a robust result. This is necessary due to the small variations in the

correction needs to be based on the variation magnitude from the initial state. This method implies that the relationship between the changes in pressure and CO_2 is independent from the initial conditions . This assumption is supported by the results of the Mesonet pressure dependence experiment that showed similar behavior for pressures higher and lower than sea level pressure. Nonetheless, to validate this assumption, the method was developed using two learning cases and then tested on two different testcases. test range created by using the ambient conditions as an initial state. If only a small sample is used to determine the coefficients, these small variations in the test range can bias the coefficients. In this section, we demonstrate an example of this technique. We used two "learning" cases to generate data points for the cubic fitting (shown in 3.1.1) and then evaluated the performance of the correction on two "test" cases.

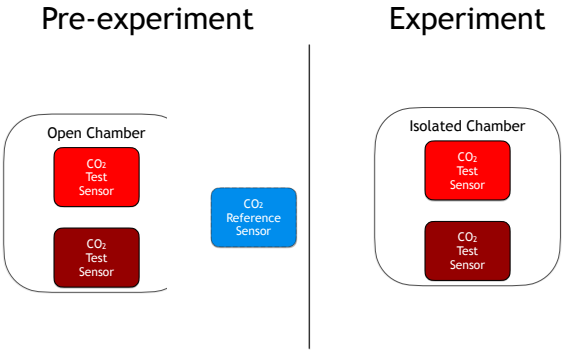

Figure 10. Diagram for the benchtop pressure correction experiment. Chamber and sensors stabilize to environment conditions (pre-experiment). Then, the chamber's isolation maintains the initial CO_2 values while pressure changes.

Since each test case is performed with two test sensors, the assumption method was evaluated four different times.

As shown in Fig. **??,** The use of only two test sensors (one test system) was determined by the size of the BACO Engineering 5-Gallon Vacuum Chamber Kit. Still, the variations in experimental conditions between all four cases used for development and evaluation have different initial pressures and CO_2 concentrations. However, all initial pressures provide insight into the method's repeatability. Nevertheless, it is important to note that the initial pressures in all tests are lower than sea level pressure. This occurs because the experiments were performed in Oklahoma (approximately 360 m above sea level). All cases emulate a typical UAS-based atmospheric CO_2 vertical profile, where there is a dwell period (in this case, 1.5 minutes) to ensure samples from the previous altitude are discarded from the system after a change in altitude.

Dataset for development and validation of the pressure correction coefficient determination method. The first row data was used to determine the coefficients for each test sensor, and the second row data was used to evaluate the performance of the coefficients. The solid black curve represents the pressure inside the chamber. The orange curves represent the CO_2

~~concentrations reported by the independent and test sensors. The black (left) and orange (right) y-axes provide the scales for pressure and CO_2, respectively.~~

~~The correction coefficients for each of the two test sensors were determined using the cubic equation fitting method from Gaynullin et al. (2016) and the data from the two cases labeled as "Learn"~~The pressure range tested emulates a flight to the average height of the top of the Atmospheric Boundary Layer in Oklahoma. The results ~~from these experiments~~ for all four cases can be seen in Fig. 11 and Tab. 5, where the time-series data for the reference, original, and corrected concentrations (for both test sensors) are plotted together for comparison. The results demonstrate ~~four instances where~~ how the low-cost coefficient determination method successfully produced errors smaller than ~~±2.5~~2.5 ppm ~~. This result is~~ in all four cases. These results are even more impressive considering the data represents emulated flights up to 5,200 ft above ground level in Oklahoma or 6,500 ft above sea level, performed in less than 30 minutes.

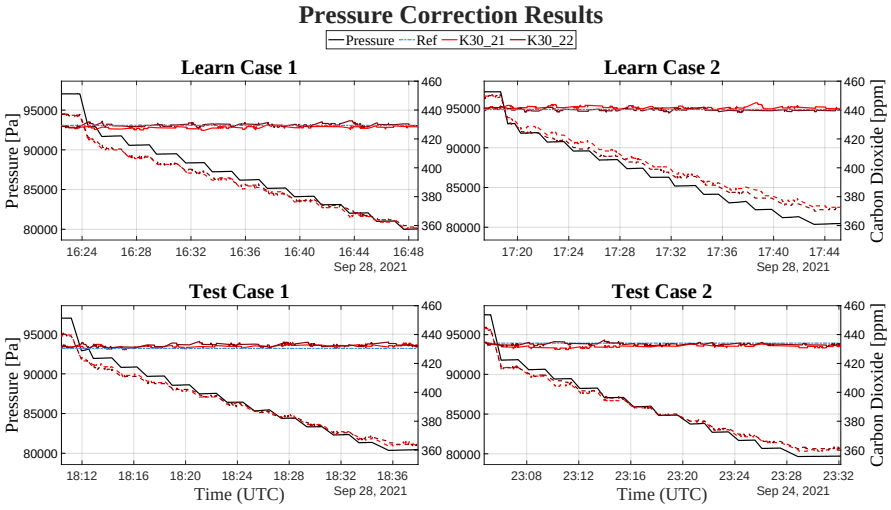

Figure 11. ~~Results from~~ Dataset for development and validation of the ~~low-cost~~ pressure correction coefficient determination ~~experiment~~method. The first row data was used to determine the coefficients for each test sensor, and the second row data was used to evaluate the performance of the coefficients. The solid black curve represents the pressure inside the chamber. The red curves represent the CO_2 values reported by test sensors (dashed lines represent the original data, and the solid lines represent the corrected data).

Table 5. Coefficients from the benchtop pressure correction method.

Sensor	k_1 *	k_2 *	k_3 *	k_4 *	R^2 *	RMSE			
						Learn 1	Learn 2	Test 1	Test 2
K30_21	-3.6254e-12	-1.5353e-07	0.0027	22.3675	0.9952	1.6650	1.7060	1.6818	2.4470
K30_22	-1.7450e-12	-6.3144e-08	0.0040	26.2825	0.9992	0.9588	0.8368	2.3899	1.0270

5 ~~Time Response to Pressure~~

4.0.1 Time Response to Pressure

While analyzing the data for the pressure correction experiment, a delay in CO_2 concentration change due to pressure change was noticed. ~~No~~ While time response to pressure, temperature, and relative humidity should have its own dedicated study, we elected to add to this article a small experiment to illustrate the time response to pressure due to its impacts being independent of sensor housing design. Another reason to add a small commentary here is to at least create awareness of its potential impact since no mention of such ~~affect~~ an effect was found in all the literature reviewed for this article. ~~Therefore, the pressure correction experimentsetup (detailed in section 3.1.1) was used again to further investigate the matter.~~

~~Using four~~ In this experiment, we used the BACO Engineering 5-Gallon Vacuum Chamber Kit to produce examples of impulses, steps, and stairs. These three distinct patterns of pressure variation ~~,~~ are shown in Fig. 12~~, the existence of a time-response to pressure was confirmed. This effect can be visualized in the fourth case , where the sharp pressure change produces an exponential response in CO_2~~.

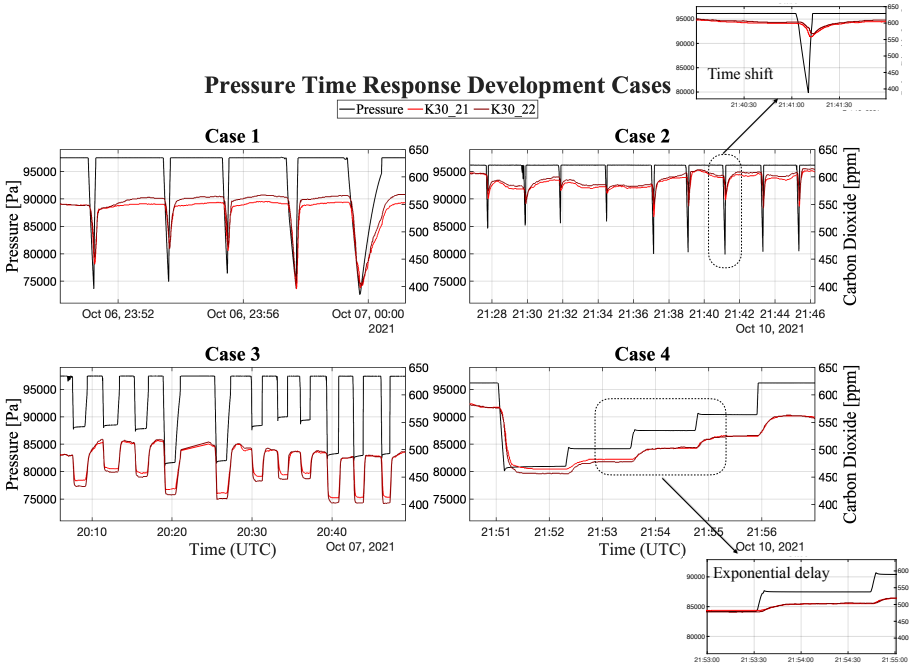

Figure 12. Development data for investigation of the pressure time-response. Cases 2 and 4 highlight the time shift and exponential delay. The solid black series represents the pressure inside the chamber for all plots. The two red series represent the CO_2 values reported by the test sensors.

Analyzing the four cases presented in Fig. 12, we noticed the effects of the time response to pressure had two components. There is a constant delay that causes a time shift (illustrated in case 2) and an exponential delay similar to an e-folding effect.

Because the pressure chamber is completely isolated from the external environment, ~~we can affirm this delay~~ once closed, we can conclude that the time response to pressure is independent of the effects of the sensor's time response to actual changes in CO_2~~concentration.~~ . This time response to pressure can introduce errors when performing pressure corrections on low-cost NDIR CO_2 sensors because fitting algorithms would map multiple distinct CO_2 values to a single pressure value. There are two strategies to mitigate this problem.

~~Development data for investigation of the pressure time-response. Cases 2 and 4 highlight the time shift and exponential delay. For all plots, the solid black series represents the pressure inside the chamber. The two orange series represent the CO_2 concentrations reported by the test sensors. The black (left) and orange (right) y-axes provide the scales for pressure and CO_2, respectively.~~

~~Perhaps the common practice of using custom~~ The first strategy is to discard CO_2 samples near pressure changes. This strategy is fairly common when post-processing data from UAS-based gas sampling that uses any sensor housing and controlled airflow~~for UAS-based gas sampling (e. g., B. H. de Azevedo, 2020) is the reason~~ . In these cases, removing samples near pressure changes is necessary because the plumbing and housing add a memory to the system. In other words, air samples from one pressure/altitude are transported by the UAS to another pressure/altitude before the samples complete their course through the plumbing and housing. Perhaps this common practice of discarding CO_2 samples near pressure changes is why this effect does not appear in the literature. ~~When employing these two techniques, a volume bigger than NDIR sensor's optical chamber is created. Therefore, when the aircraft changes altitude, the first samples at the new altitude need to be discarded. This common practice avoids errorssuch as gradient blurring. Albeit, unintentionally, this practice would also mitigate this pressure time response error from the pressure correction algorithm. Nonetheless, we used the data from the two test cases for the pressure correction to evaluate if a pressure time response correction could be developed.~~

~~The error correction was performed in two parts. First, we used an exponential correction, also known as an e-folding correction~~The second strategy is to correct the time-response induced errors before correcting the pressure-induced errors. Since no mentions of this error were found in the reviewed literature, no correction methods were found either. Therefore, we attempted to correct this error using known techniques for other atmospheric sensors, following the time response modeling from Houston and Keeler (2018) and Miloshevich et al. (2004). ~~The time constant~~ We used the steps and stairs (cases 3 and 4) to calculate an averaged constant (τ) for the exponential correction ~~was estimated from the data in development cases 3 and 4. Finally, we applied a constant time shift on the data. The shift constant was estimated from development~~ and the peak distances of the impulses (cases 1 and ~~2. The results for our correction attempts are shown in Fig. 13 and ??~~. 2) for the averaged shift.

To evaluate the ~~impact of the correction attempt, an idealized signal~~ performance of this correction method, we created an artificial signal to represent the ideal response to pressure. This artificial signal represents what the sensor response to pressure should have been without the pressure time-response error. In this artificial signal, the pressure-induced error is instantaneously reflected on the sensor output. Such a signal would minimize (or not produce) the mapping of multiple distinct CO_2 values to a single pressure value during the curve fitting algorithm for the pressure correction method. Therefore, this artificial signal represents the benchmark for a pressure time-response correction method. The artificial signal representing the ideal response to pressure was created using the timestamps of the pressure changes and the average CO_2 concentration for each pressure

level. ~~The~~ This average CO_2 concentration was obtained for each pressure level after all exponential delays. The results of our correction attempt are shown in Fig. 13.

Our proposed correction method ~~was able to improve~~ improved the mean absolute error (MAE) for both sensor units, when compared to the ~~idealized~~ artificial signal. MAE for Sensor 1 improved from 0.9806 to 0.6633 ppm, and Sensor 2 improved from 0.8702 to 0.5940 ppm. The improvements are even more expressive when we analyze the maximum absolute error (MxAE). Sensor 1 improved from $MxAE = 12.965$ to 5.3024 ppm and Sensor 2 improved from $MxAE = 11.533$ to 4.4393 ppm. The experiment was repeated on another test case with similar results (see supplement S19).

~~Unfortunately, the attempted correction was not as effective on the gradual pressurechanges. For example,~~ Although the results presented here indicate the feasibility of a repeatable method to correct pressure time-response errors on low-cost NDIR CO_2 sensors, we highlight again our intention to only create awareness of this potential source of error. As mentioned above, the time response to pressure, temperature, and relative humidity should have its dedicated study. Despite improving MAE and MxAE, our proposed correction still presented errors. Most notably during the period from 18:26 to 18:32, ~~shown~~ highlighted on the time series for Sensor 2 ~~on the Test Case 1~~ (Fig. 13). ~~However, as mentioned before, this error will not appear in most applications, and it can be mitigated by discarding initial samples for each altitude. For those who~~ For those whom this time response ~~may be~~ is an issue, we recommend repeating these experiments on a better quality chamber~~. One~~, one capable of producing smaller and better-defined pressure changes~~. The solenoid-base control for the~~, or adopting the first mitigation strategy presented in this section.

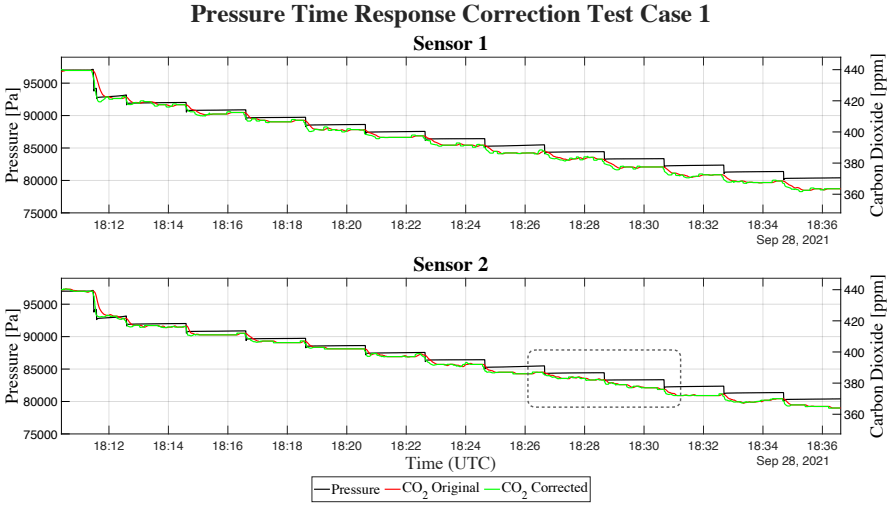

Figure 13. Correction Results for Test Case 1 for the sensor's time response to pressure changes. The solid black curve represents the pressure inside the chamber. The red and green curves represent the test sensor's original and corrected CO_2 values.

4.1 Temperature and Relative Humidity

In this section, we investigate four low-cost ~~BACO Engineering 5-Gallon Vacuum Chamber Kit~~ benchtop setups to characterize and correct the impact of temperature and relative humidity on low-cost NDIR CO_2 sensors. For these experiments, we are considering the combined effects of temperature and relative humidity due to the difficulty of isolating them in a benchtop setting. As mentioned in section 4, the goal is to devise practical methods for field calibrations. In all four experiments, the test sensors were compared to a reference gas analyzer (LI-840A or LI-820), and the thermodynamic sensor package for UAS measurements described in B. H. de Azevedo (2020) was used to monitor the experimental conditions. This thermodynamic sensor package consists of three IMET glass bead thermistors and three IST HYT-271 hygrometers. In the cases where the test sensors used sensor housing, the HYT-271 hygrometer inside the sensor housing was used to compare the experiment's temperature and relative humidity to the values inside the housing. For more information on the test sensor configuration and housings used, refer to section 2.1.

The first benchtop setup tested was a large plastic container with an electric heater and a water spray. Inside the container were the UAS thermodynamic sensor package, a medium mixing fan, and the reference and test sensors. In this setup, the container (open lid) was placed near an open window and two large fans. After the temperature, relative humidity, and CO_2 levels were stable, an experiment operator partially closed the lid and activated either the heater or the water spray. Our initial assessment indicates that the large fans were not able to mitigate the impact of the CO_2 produced by the proximity of the operator and the test sensors. To mitigate the impacts of the operator, we also attempted to reduce the experiment's duration and intensify the test variable stimulus, similar to the pressure impulse shown in Fig. 12. In this short duration format, the UAS thermodynamic sensor package registered the short stimulus (for temperature and relative humidity). However, the same was not confirmed by the HYT-271 sensors inside the K30 housings, and the CO_2 test sensors did not produce ~~data with enough quality to investigate the matter further.~~ a coherent response. Even though the UAS thermodynamic sensor package and the pump intake for the reference and test sensors were placed a few centimeters apart, the approximately 68 L (18 gal) of the container may have been too large for the short stimulus to produce a relevant change inside the K30 sensor housings. An example of the results produced by this setup can be seen in this article's supplement (Fig. S20).

In the second benchtop setup tested, we removed the large plastic container and allowed the room with the reference and test sensors to stabilize to constant levels of pressure, temperature, relative humidity, and CO_2. With a long extension cord, we allowed the electric heater to simultaneously warm-up in a separate room. Then we moved the electric heater to the test room and placed it immediately in front of the reference and test sensors. In this experiment (panels B and C in Fig. 14), we colocated all six test sensors in all three test configurations (see Sec. 2.1). An example of the results produced by this setup can be seen in this article's supplement (Fig. S21). Again, the HYT-271 sensors inside the housed test systems did not indicate the same temperature and relative humidity changes as the UAS thermodynamic sensor package. Nonetheless, the behavior of the housed test sensors was similar to the unhoused sensors (except for the sensor noise caused by temperature on the unhoused test sensor K30_13).

The third benchtop setup tested used a small plastic container (approx. 12 L). Inside the container were the UAS thermodynamic sensor package, the test sensors, and a small mixing fan. Due to the container size, we could only use four test sensors in this setup, and the reference sensor had to be placed outside the plastic container. To maintain reference colocation, we used

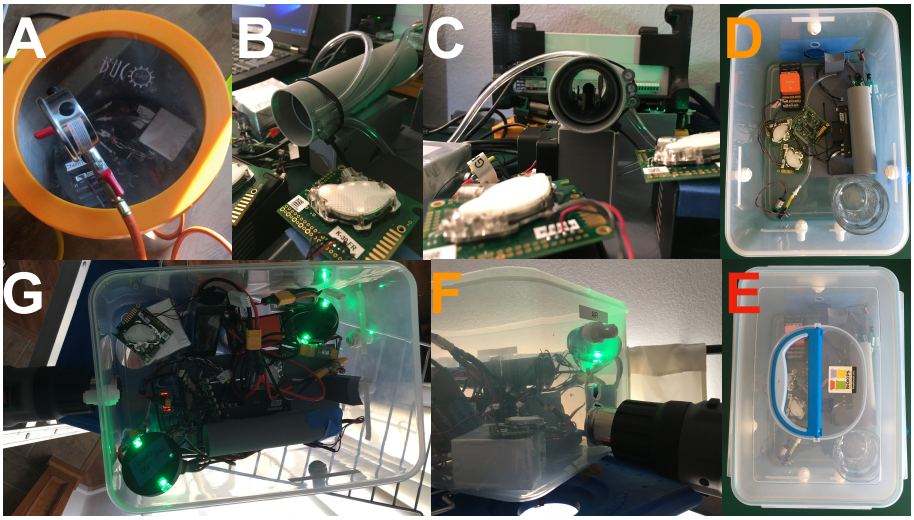

Figure 14. ~~Correction Results for Test Case 1 for~~ Benchtop experiments to characterize and mitigate the impacts of pressure~~time response~~, temperature, and relative humidity on low-cost NDIR sensors. ~~The solid black curve represents~~ Panel A shows the Baco Engineering pressure ~~inside the~~ chamber. The ~~grey and orange curves~~ remaining panels represent the ~~original~~ second (B and ~~corrected CO_2 concentrations reported by the test sensor. The black~~ C), third (~~left~~D and E), and ~~orange~~ fourth (~~right~~F and G) ~~y-axes provide the scales for pressure~~ benchtop temperature and CO_2, ~~respectively~~relative humidity experimental setups.

a plumbing port to allow the reference sensor to sample air from inside the container (panels F and G in Fig. 14). At the beginning of the experiment, the container's lid was open, and all the sensors were allowed to stabilize to the room levels of pressure, temperature, and relative humidity. Then, the container lid was closed, and an electric heater was turned on. After five minutes, the heater was turned off, and the lid was opened. All four test sensors (both housed and unhoused) responded to the increase in temperature. However, the reference also presented a slight increase in CO_2 for the same period. An example of the results produced by this setup can be seen in Fig. 15.

~~In this article, we validated previous results in the literature and produced new results that support the general robustness of~~

The fourth and final benchtop setup tested used the same arrangement from the previous setup, with the heater being replaced with a glass for boiling water (panels D and E in Fig. 14). Again, the container's lid was open, and all the sensors were allowed to stabilize to the room levels of pressure, temperature, and relative humidity. Then, the boiling water was added to the glass, and the container's lid was closed. After eight minutes, the lid was opened. This setup's results can be seen in Fig. 16. All four test sensors (both housed and unhoused) responded to the increase in temperature and relative humidity, while the reference sensor did not indicate a change in CO_2.

The results from experiment setups three and four are encouraging. However, repeated executions of both showed some variation on how much and how fast the test sensors reflected the chamber conditions. Also, potential contamination from the experiment's operator opening and closing the container lid make it less consistent. Therefore, we limit the analyses of these results to indicate only that a low-cost, low-complexity method can be developed for field calibrations of low-cost NDIR CO_2

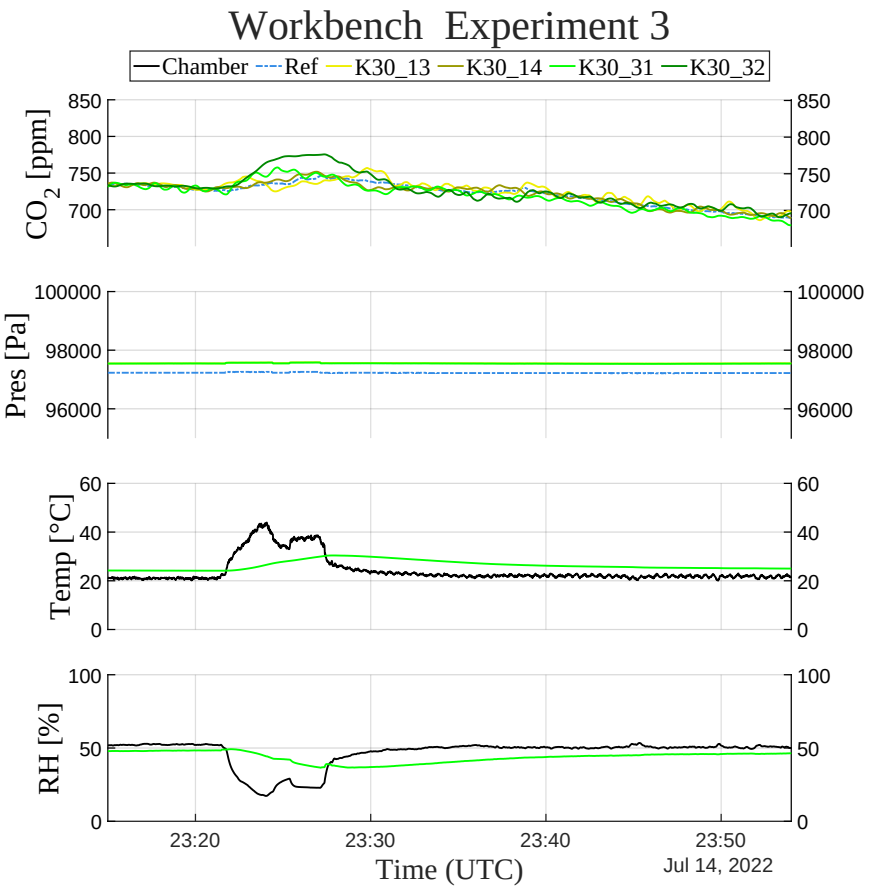

Figure 15. ~~Correction~~ Results for ~~Test Case 2 for pressure time response. The solid black curve represents~~ the ~~pressure inside the chamber~~third benchtop setup tested. The ~~grey and orange curves represent~~ top panel shows the ~~original and corrected~~ reported CO_2 ~~concentrations reported by~~ values for all sensors, the ~~test sensor. The black~~ following panels show the experimental conditions (~~left)~~ pressure, temperature, and ~~orange (right~~relative humidity) ~~y-axes provide the scales~~ for ~~pressure~~ the reference and ~~CO_2, respectively~~test systems.

sensors. A broader discussion of the general considerations for testing low-cost NDIR ~~sensors. More importantly~~CO_2 sensors is presented in the following section.

5 Discussion

In this article, we presented ~~a low-cost benchtop correction procedure to considerably improve the accuracy of CO_2 measurements to be within ± 2.5 . These findings support the use of~~ many different chambered and benchtop low-complexity experiments in hopes of exploring the behavior of low-cost NDIR CO_2 sensors under the strong rates of changes in pressure, temperature,

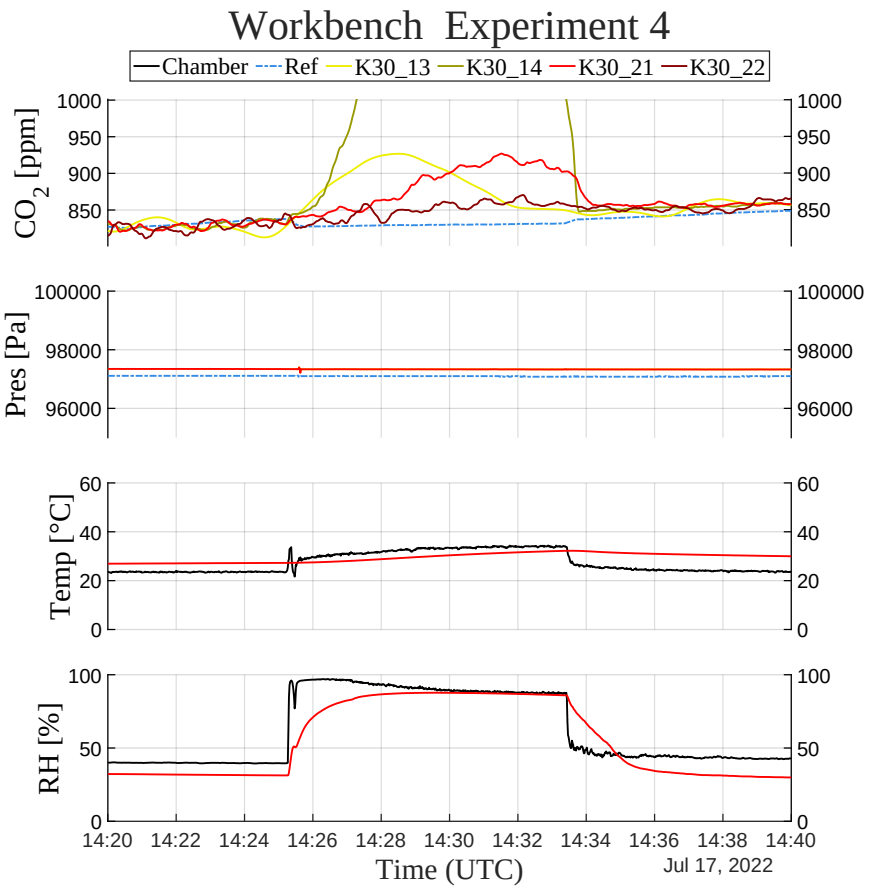

Figure 16. Results for the fourth benchtop setup tested. The top panel shows the reported CO_2 values for all sensors. The following panels show the experimental conditions (pressure, temperature, and relative humidity) for the reference and test systems.

and relative humidity commonly associated with UAS-based measurements. In our total time working with these sensors, we noticed some characteristics worth highlighting in this section. The first characteristic worth discussing is the sensor's construction. The Senseair K30 and all other low-cost NDIR ~~sensors~~ CO_2 sensors commercially available were not designed for UAS-based ~~atmospheric measurements as a complementary in-situ tool for many scientific applications.~~

~~This article also produced important results regarding the isolated impact of each of the three variables tested. Even though the results in this article did not support a direct dependence between the reported concentrations~~applications. Many of them were designed for indoor, medical, and industrial applications. This design assumes a natural air exchange with the environment over a long period (minutes to hours). Therefore, their optical chambers offer little control over the air entering and exiting the chamber. This long and uncertain permeation period directly impacts the spatiotemporal resolution of UAS-based

measurements with these sensors. To mitigate this permeation issue, some researchers and manufacturers adopt fans or custom airflow solutions with diaphragm pumps (e.g., CO2Meter's pump cap for the K30).

Even though we did not study the impacts of airflow control solutions on the sensors and their responses to pressure, temperature, and ~~humidity, minor impacts from these variables cannot be ruled out. Future characterization and validation work should investigate a~~ relative humidity, the difference in results between the chambered and benchtop experiments indicates a possible impact. This seemed more evident in the temperature experiments, as most of our attempts to generate impulse-like responses failed, and our longer transitions worked. Similar errors in temperature and relative humidity probes associated with filters and airflow have been reported in the literature (e.g., Richardson et al., 1998). This characteristic limited our experiments of changes in temperature and relative humidity to intervals between 5 and 10 minutes. However, this potential limitation is not considered a problem for UAS-based applications using these low-cost ~~setup using NIST traceable canisters with known concentration to control CO_2 conditions during the experiments~~NDIR CO_2 sensors because the oversampling techniques necessary to improve their accuracy and CO_2 time-response already require slower flight speeds.

~~In the particular case of temperature dependence, we also recommend expanding the isolated experiments done in this article to cover low temperatures. The test sensors used here, the~~ Another interesting effect noticed during the study was the impact of radio frequency on the sensor's reported values. To keep the chamber and benchtop arrangements as simple as possible, we avoided using complementary computers to log the data from the sensors. Instead, we used the sensors in their flight package format, completely independent from external resources. This choice reduced the complexities of running power and data cables to the chambers and benchtop setups. This choice also better reflected how the sensors were expected to behave and provide data during flights. The GPS and flight telemetry modules used to time-position stamp the CO_2 data and transmit it, in near real-time, to the ground-station computer produce electromagnetic interference (EMI) on the K30 ~~, are rated for operations from 0 to 50 , but other sensors within the~~ sensors. This EMI generates oscillations of the reported CO_2 values in the order of hundreds of ppm. Even though this effect can be mitigated with proper grounding and by adding EMI tape to the sensor's airflow control housing, this effect impacted our ability to colocate sensors in some experimental setups. This was particularly impactful for the unhoused control sensors inside the BACO Engineering benchtop pressure chamber and the small plastic container for the benchtop temperature and relative humidity experiments. A video of this EMI effect is provided in this article's video supplement section.

Finally, it is important to highlight that the low-complexity methods shown in this study are very sensitive to changes in background CO_2. This sensitivity comes from using reference gas analyzers as the true CO_2 values. This use of an external reference implies the constant comparison of the values reported by the test sensors and the reference gas analyzer. However, the sensitivity to CO_2 changes of these two different categories of sensors differs considerably. Therefore, obfuscating the impacts of the environmental test variable. Thus, any repetition of the methods shown in this article requires an environment with small to no changes in CO_2 conditions. As mentioned previously, these conditions can be achieved by isolating the environment and reducing the experiment's duration.

6 Conclusions

In this article, we reviewed the main concerns regarding the use of commercial low-cost ~~NDIR category have broader ranges. Therefore, continuing to expand the test range and repeating these experiments with other low-cost~~ NDIR ~~sensor models will increase accuracy and trust in~~ sensors for atmospheric CO_2 measurements found in the literature. We then built upon experimental results in the literature by investigating the isolated impact of pressure, temperature, and relative humidity under emulated UAS flight conditions. We presented a new dataset with stronger rates of change than previously found in the literature and a low-complexity method using a reference gas analyzer. This low-complexity method successfully produced error correction algorithms for each studied variable within a few ppm of the more expensive reference sensors. Even though we were not able to successfully demonstrate the low-cost benchtop setups to characterize and mitigate the impact of these variables on the same sensors, this article provides important insights for the future development of these setups. We believe these low-complexity procedures are a way to lower the entry barriers to this research field while improving the accuracy of UAS-based ~~measurements done with them~~CO_2 measurements through frequent recalibration.

~~It is also important to~~ Another important contribution of this study is to raise awareness around other issues associated with UAS-specific deployment of low-cost NDIR CO_2 sensors, in particular the potential impacts of these sensors' time response to pressure, temperature, and relative humidity. We strongly believe these issues should have their own dedicated study. We also recommend the investigation of the impact of custom airflow control solutions on the propagation of temperature through the measurement system.

Finally, we note that the statements from Gaynullin et al. (2016) ~~,~~regarding the need for a distinct set of correction coefficients for each sensor were verified in this study. This requirement is also supported by Martin et al. (2017), who found that a generalized set of coefficients could make the accuracy worse than ~~uncorrected accuracy~~when uncorrected.

In our concluding remarks, we ~~would like to~~ emphasize the importance of sensor placement, sensor housing design, ~~airflow control to~~ and airflow control for successful UAS-based measurements. Furthermore, the characterization of UAS-based systems should ~~take into account~~ consider the potential contamination introduced by the aircraft and its mode of operation (e.g., vertical profile, transects, hover, and other flight patterns). Finally, any system used to support long-term research or forecast operations should also account for temporal drift and sensor decay.

Video supplement. https://youtu.be/4rYWESlXOTc

Author contributions. This study was conceptualized by GBHA and DS. The methodology was designed by GBHA and DS. The Mesonet experiments were designed by GBHA and CAF. The Benchtop experiments were designed by GBHA, DS, and BD. The formal analysis and post-processing of the data were carried out by GBHA under the supervision of DS. Supporting software was developed by GBHA, DS, and BD. The original draft was written by GBHA and reviewed and edited by GBHA, DS, BD, and CAF.

7

Examples of low-cost NDIR sensors *Manufacturer*Vaisala*SenseairELTKoreaGEAmphenol*CozirCo.Digital Co.SensingAdvanced SensorsModelGMM222CK30S100AN100T6615T6613CozIR-A 10,000Measurement range 0–20000–50000–100000–50000–100000–2 ±30±30±50±200±75±30±50Weight 22017102917-20Cost -95.00--104.8199.72109.00

705 7

Literature search arrangements Search stringResults+CO2 +unmanned +aerial11,300+CO2 +unmanned +aerial +(K30 OR K-30 OR "K-30")67+CO2 +unmanned +aerial +(GMM222C OR S100 OR AN100 OR T6615) -(K30 OR K-30 OR "K 30")6+Carbon +dioxide +unmanned +aerial10,500+Carbon +dioxide +unmanned +aerial +(K30 OR K-30 OR "K 30")62+Carbon +dioxide +unmanned +aerial +(GMM222C OR S100 OR AN100 OR T6615) -(K30 OR K-30 OR "K 30")3+Carbon +dioxide
710 +remotely +piloted +aircraft1520+Carbon +dioxide +remotely +piloted +aircraft +(K30 OR K-30 OR "K 30")7+Carbon +dioxide +remotely +piloted +aircraft +(GMM222C OR S100 OR AN100 OR T6615) -(K30 OR K-30 OR "K 30")1

Competing interests. The authors declare that they have no conflicts of interest.

Acknowledgements. The authors would like to recognize the efforts of David L. Grimsley, the manager of the Oklahoma Mesonet Calibration Laboratory, for his technical support during the Mesonet chamber experiments. The authors would like thank Dr.Jacob from the Unmanned
715 Systems Research Institute at the Oklahoma State University, for providing the LI-COR LI-820 reference gas analyzer used in the Mesonet chamber experiments. The authors also thank RMSA for the thorough grammatical revisions. This study was supported in part by the Vice President for Research and Partnerships (VPRP) of the University of Oklahoma OU. Publication was supported by the University of Oklahoma Libraries.

References

Al-Hajjaji, K., Ezzin, M., Khamdan, H., Hassani, A. E., and Zorba, N.: Design, development and evaluation of a UAV to study air quality in Qatar, arXiv preprint arXiv:1709.05628, 2017.

Arzoumanian, E., Vogel, F. R., Bastos, A., Gaynullin, B., Laurent, O., Ramonet, M., and Ciais, P.: Characterization of a commercial lower-cost medium-precision non-dispersive infrared sensor for atmospheric CO_2 monitoring in urban areas, Atmospheric Measurement Techniques, 12, 2665–2677, https://doi.org/10.5194/amt-12-2665-2019, 2019.

Ashraf, S., Mattsson, C. G., Thungström, G., Gaynullin, B., and Rödjegård, H.: Evaluation of a CO_2 sensitive thermopile with an integrated multilayered infrared absorber by using a long path length NDIR platform, in: 2018 IEEE International Instrumentation and Measurement Technology Conference (I2MTC), pp. 1–6, https://doi.org/10.1109/I2MTC.2018.8409758, 2018.

B. H. de Azevedo, G.: Spatially-temporally resolved sampling system for carbon dioxide concentration in the atmospheric boundary layer : a low-cost UAS approach., 2020.

Barbieri, L., Kral, S. T., Bailey, S. C. C., Frazier, A. E., Jacob, J. D., Reuder, J., Brus, D., Chilson, P. B., Crick, C., Detweiler, C., Doddi, A., Elston, J., Foroutan, H., González-Rocha, J., Greene, B. R., Guzman, M. I., Houston, A. L., Islam, A., Kemppinen, O., Lawrence, D., Pillar-Little, E. A., Ross, S. D., Sama, M. P., Schmale, D. G., Schuyler, T. J., Shankar, A., Smith, S. W., Waugh, S., Dixon, C., Borenstein, S., and de Boer, G.: Intercomparison of Small Unmanned Aircraft System (sUAS) Measurements for Atmospheric Science during the LAPSE-RATE Campaign, Sensors, 19, https://doi.org/10.3390/s19092179, 2019.

Cartier, K. M. S.: Human activity outpaces volcanoes, asteroids in releasing deep carbon, Eos, 100, 2019.

Chen, S., Yamaguchi, T., and Watanabe, K.: A simple, low-cost non-dispersive infrared CO_2 monitor, in: 2nd ISA/IEEE Sensors for Industry Conference, pp. 107–110, https://doi.org/10.1109/SFICON.2002.1159816, 2002.

Gaynullin, B., Bryzgalov, M., Hummelgård, C., and Rödjegard, H.: A practical solution for accurate studies of NDIR gas sensor pressure dependence. Lab test bench, software and calculation algorithm, in: 2016 IEEE SENSORS, pp. 1–3, https://doi.org/10.1109/ICSENS.2016.7808828, 2016.

Gibson, D. and MacGregor, C.: A Novel Solid State Non-Dispersive Infrared CO_2 Gas Sensor Compatible with Wireless and Portable Deployment, Sensors, 13, 7079–7103, 2013.

Hemingway, B. L., Frazier, A. E., Elbing, B. R., and Jacob, J. D.: Vertical Sampling Scales for Atmospheric Boundary Layer Measurements from Small Unmanned Aircraft Systems (sUAS), Atmosphere, 8, https://doi.org/10.3390/atmos8090176, 2017.

Houston, A. L. and Keeler, J. M.: The Impact of Sensor Response and Airspeed on the Representation of the Convective Boundary Layer and Airmass Boundaries by Small Unmanned Aircraft Systems, Journal of Atmospheric and Oceanic Technology, 35, 1687 – 1699, https://doi.org/10.1175/JTECH-D-18-0019.1, 2018.

Kiefer, C. M., Clements, C. B., and Potter, B. E.: Application of a Mini Unmanned Aircraft System for In Situ Monitoring of Fire Plume Thermodynamic Properties, Journal of Atmospheric and Oceanic Technology, 29, 309–315, https://doi.org/10.1175/JTECH-D-11-00112.1, 2012.

Kunz, M., Lavric, J., Gerbig, C., Tans, P., Neff, D., Hummelgärd, C., Martin, H., Rödjegård, H., Wrenger, B., and Heimann, M.: COCAP: A carbon dioxide analyser for small unmanned aircraft systems, Atmos. Meas. Tech., 11, 1833–1849, https://doi.org/10.5194/amt-11-1833-2018, 2018.

Martin, C. R., Zeng, N., Karion, A., Dickerson, R. R., Ren, X., Turpie, B. N., and Weber, K. J.: Evaluation and environmental correction of ambient CO_2 measurements from a low-cost NDIR sensor, Atmospheric Measurement Techniques, 10, 2383–2395, https://doi.org/10.5194/amt-10-2383-2017, 2017.

McPherson, R. A., Fiebrich, C. A., Crawford, K. C., Kilby, J. R., Grimsley, D. L., Martinez, J. E., Basara, J. B., Illston, B. G., Morris, D. A., Kloesel, K. A., Melvin, A. D., Shrivastava, H., Wolfinbarger, J. M., Bostic, J. P., Demko, D. B., Elliott, R. L., Stadler, S. J., Carlson, J. D., and Sutherland, A. J.: Statewide Monitoring of the Mesoscale Environment: A Technical Update on the Oklahoma Mesonet, Journal of Atmospheric and Oceanic Technology, 24, 301–321, https://doi.org/10.1175/JTECH1976.1, 2007.

Miloshevich, L. M., Paukkunen, A., Vömel, H., and Oltmans, S. J.: Development and Validation of a Time-Lag Correction for Vaisala Radiosonde Humidity Measurements, Journal of Atmospheric and Oceanic Technology, 21, 1305 – 1327, https://doi.org/10.1175/1520-0426(2004)021<1305:DAVOAT>2.0.CO;2, 2004.

Mitchell, T., Kidd, J., and Jacob, J. D.: Wildfire Plume Tracking and Dynamics Using UAS with In-Situ CO_2 Measurements, AIAA SciTech Forum, 4, 2016.

Mizoguchi, Y. and Ohtani, Y.: Comparison of response characteristics of small CO2 sensors and an improved method based on the sensor response, Journal of Agricultural Meteorology (Japan), 2005.

Nelson, K. N., Boehmler, J. M., Khlystov, A. Y., Moosmuller, H., Samburova, V., Bhattarai, C., Wilcox, E. M., and Watts, A. C.: A Multi-pollutant Smoke Emissions Sensing and Sampling Instrument Package for Unmanned Aircraft Systems: Development and Testing, Fire, 2, 32, 2019.

Pandey, S. K. and Kim, K.-H.: The Relative Performance of NDIR-based Sensors in the Near Real-time Analysis of CO_2 in Air, Sensors, 7, 1683–1696, https://doi.org/10.3390/s7091683, 2007.

Piedrahita, R., Xiang, Y., Masson, N., Ortega, J., Collier, A., Jiang, Y., Li, K., Dick, R. P., Lv, Q., Hannigan, M., and Shang, L.: The next generation of low-cost personal air quality sensors for quantitative exposure monitoring, Atmospheric Measurement Techniques, 7, 3325–3336, https://doi.org/10.5194/amt-7-3325-2014, 2014.

Richardson, S. J., Frederickson, S. E., Brock, F. V., and Brotzge, J. A.: Combination temperature and relative humidity probes: Avoiding large air temperature errors and associated relative humidity errors, in: Preprints, 10th Symposium on Meteorological Observations and Instrumentation, Phoenix, AZ, American Meteorological Society, vol. 278, p. 283, 1998.

Stephens, B. B., Miles, N. L., Richardson, S. J., Watt, A. S., and Davis, K. J.: Atmospheric CO_2 monitoring with single-cell NDIR-based analyzers, Atmospheric Measurement Techniques, 4, 2737–2748, https://doi.org/10.5194/amt-4-2737-2011, 2011.

Villa, T. F., Gonzalez, F., Miljievic, B., Ristovski, Z. D., and Morawska, L.: An Overview of Small Unmanned Aerial Vehicles for Air Quality Measurements: Present Applications and Future Prospectives, Sensors, 16, https://doi.org/10.3390/s16071072, 2016.

Watai, T., Machida, T., Ishizaki, N., and Inoue, G.: A Lightweight Observation System for Atmospheric Carbon Dioxide Concentration Using a Small Unmanned Aerial Vehicle, Journal of Atmospheric and Oceanic Technology, 23, 700 – 710, https://doi.org/10.1175/JTECH1866.1, 2006.

Yasuda, T., Yonemura, S., and Tani, A.: Comparison of the Characteristics of Small Commercial NDIR CO_2 Sensor Models and Development of a Portable CO_2 Measurement Device, Sensors, 12, 3641–3655, https://doi.org/10.3390/s120303641, 2012.

Yasuda, Y., Ohtani, Y., Mizoguchi, Y., Nakamura, T., and Miyahara, H.: Development of a CO_2 gas analyzer for monitoring soil CO_2 concentrations, Journal of forest research, 13, 320, 2008.